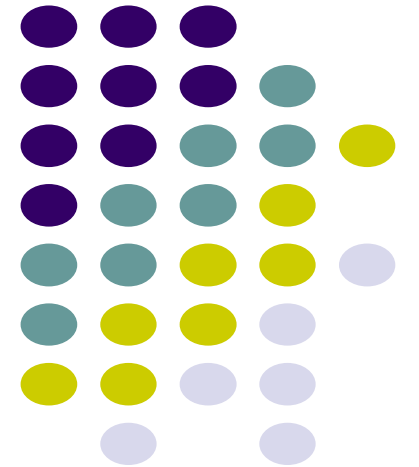


Filtering in the Frequency Domain (Applications)

Dr. Navjot Singh
Image and Video Processing

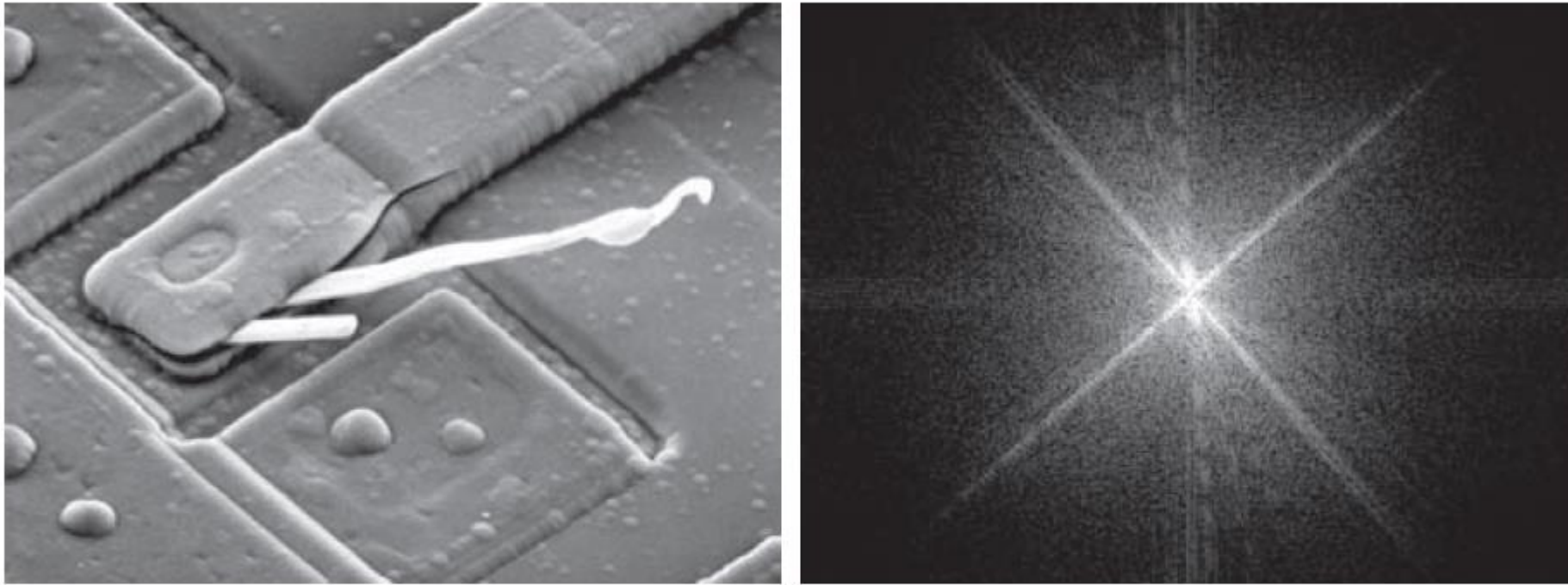
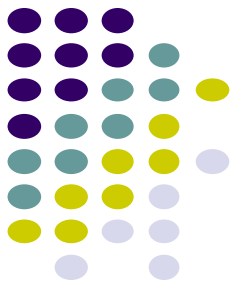




Acknowledgements

- Gonzalez, Rafael C. Digital image processing. Pearson, 4th edition, 2018.
- Jain, Anil K. Fundamentals of digital image processing. Prentice-Hall, Inc., 1989.
- Digital Image Processing course by Brian Mac Namee, Dublin Institute of Technology
- Digital Image Processing course by Christophoros Nikou, University of Ioannina

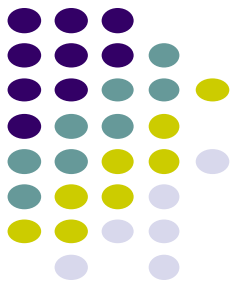
The Basic Filtering in Frequency Domain



a b

FIGURE 4.28 (a) SEM image of a damaged integrated circuit. (b) Fourier spectrum of (a). (Original image courtesy of Dr. J. M. Hudak, Brockhouse Institute for Materials Research, McMaster University, Hamilton, Ontario, Canada.)

The Basic Filtering in Frequency Domain (contd.)



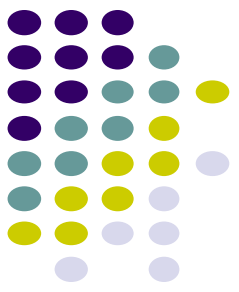
- Modifying the Fourier transform of an image
- Computing the inverse transform to obtain the processed result

- $$g(x, y) = \mathfrak{F}^{-1}\{H(u, v)F(u, v)\}$$

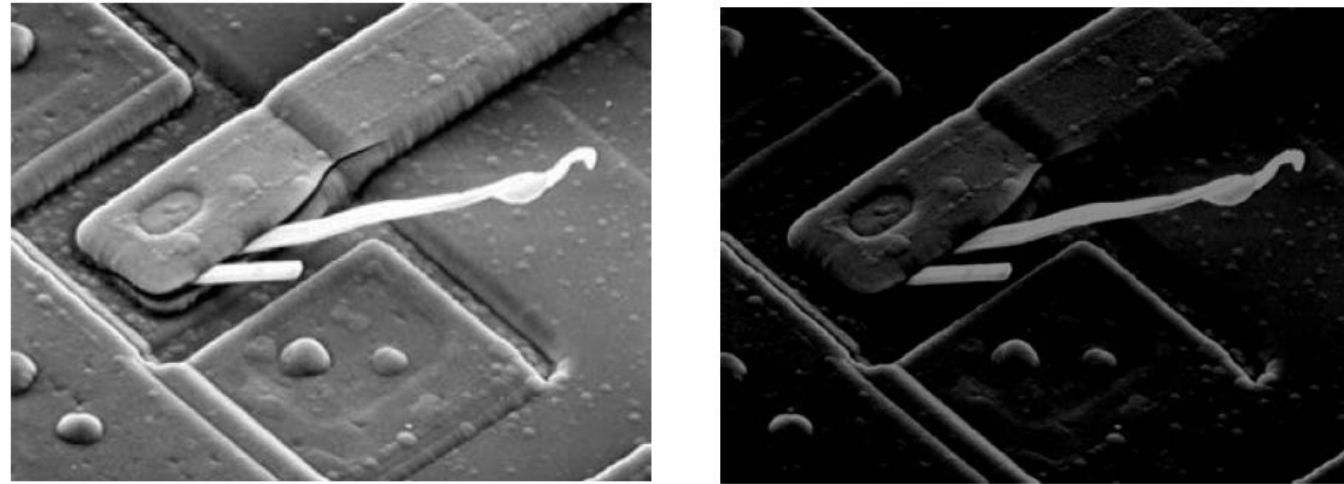
$F(u, v)$ is the DFT of the input image

$H(u, v)$ is a filter function.

The Basic Filtering in Frequency Domain (contd.)

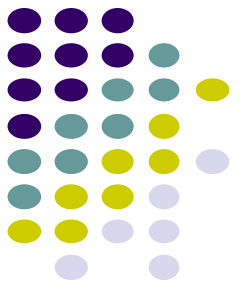
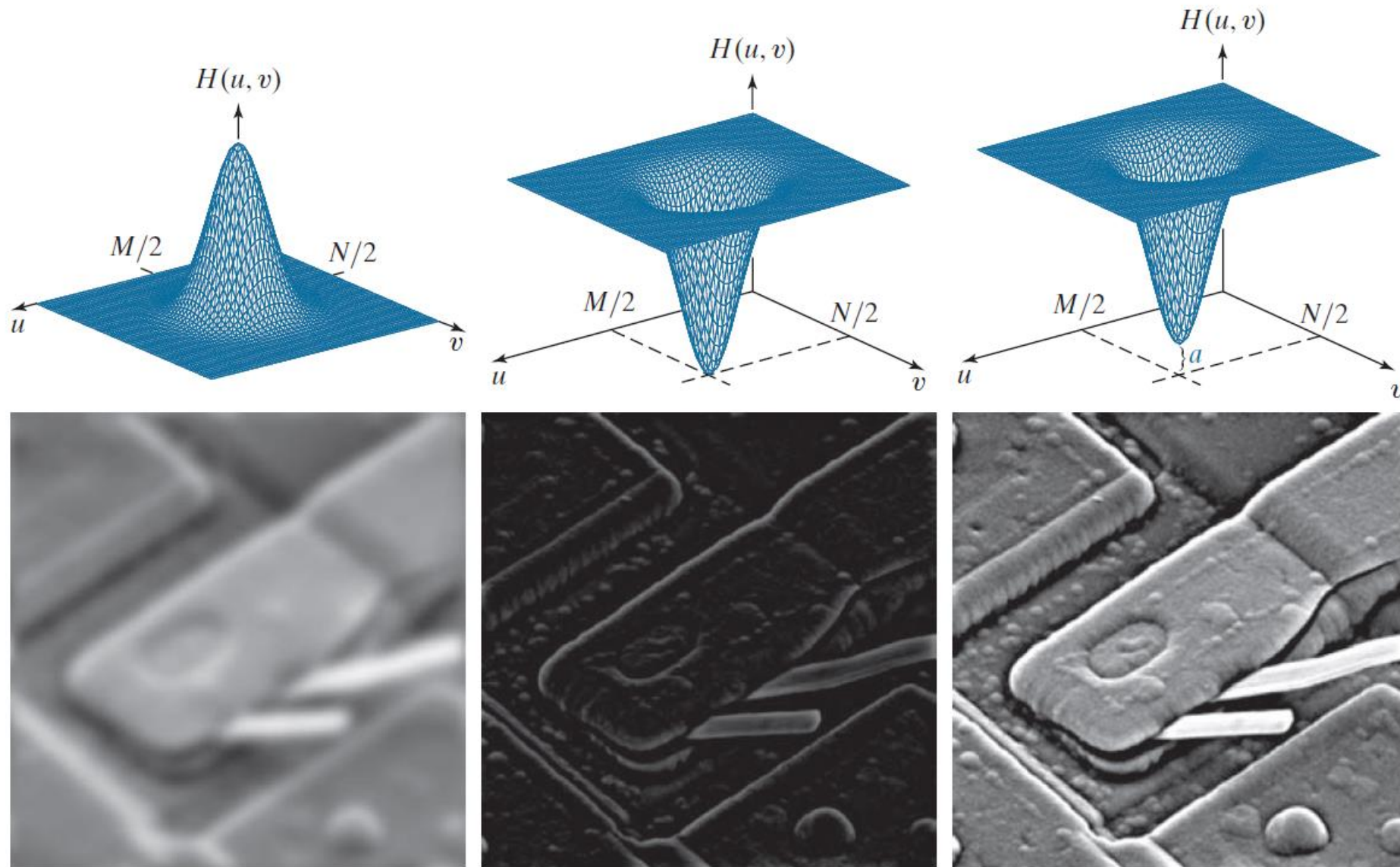


- In a filter $H(u,v)$ that is 0 at the center of the transform and 1 elsewhere, what's the output image?



a b

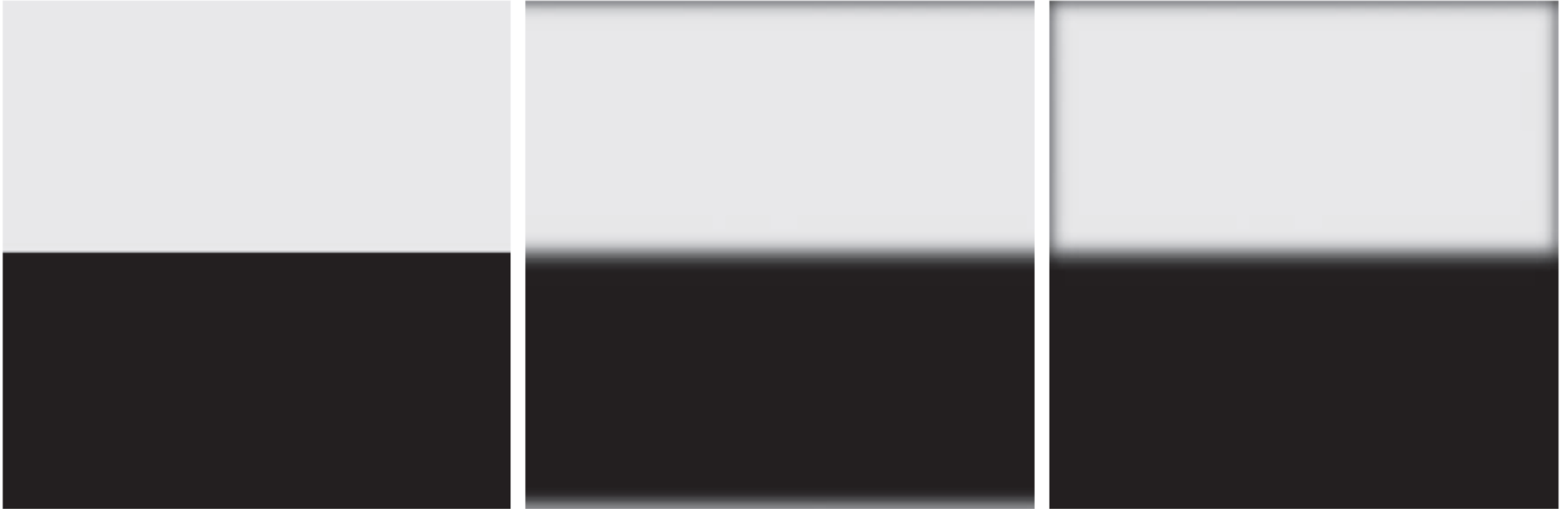
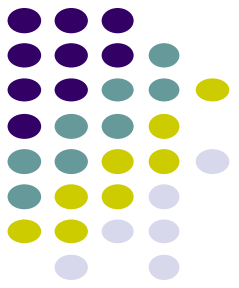
FIGURE 4.29 (a) SEM image of a damaged integrated circuit. (b) Fourier spectrum of (a). (Original image courtesy of Dr. J. M. Hudak, Brockhouse Institute for Materials Research, McMaster University, Hamilton, Ontario, Canada.)



a	b	c
d	e	f

FIGURE 4.30 Top row: Frequency domain filter transfer functions of (a) a lowpass filter, (b) a highpass filter, and (c) an offset highpass filter. Bottom row: Corresponding filtered images obtained using Eq. (4-104). The offset in (c) is $a = 0.85$, and the height of $H(u, v)$ is 1. Compare (f) with Fig. 4.28(a).

The Basic Filtering in Frequency Domain (contd.)



a b c

FIGURE 4.31 (a) A simple image. (b) Result of blurring with a Gaussian lowpass filter without padding. (c) Result of lowpass filtering with zero padding. Compare the vertical edges in (b) and (c).

Zero-Phase-Shift Filters



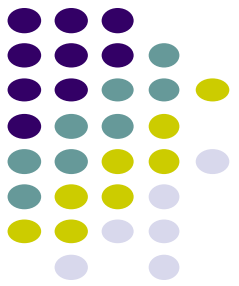
$$g(x, y) = \mathfrak{T}^{-1} \{ H(u, v) F(u, v) \}$$

$$F(u, v) = R(u, v) + jI(u, v)$$

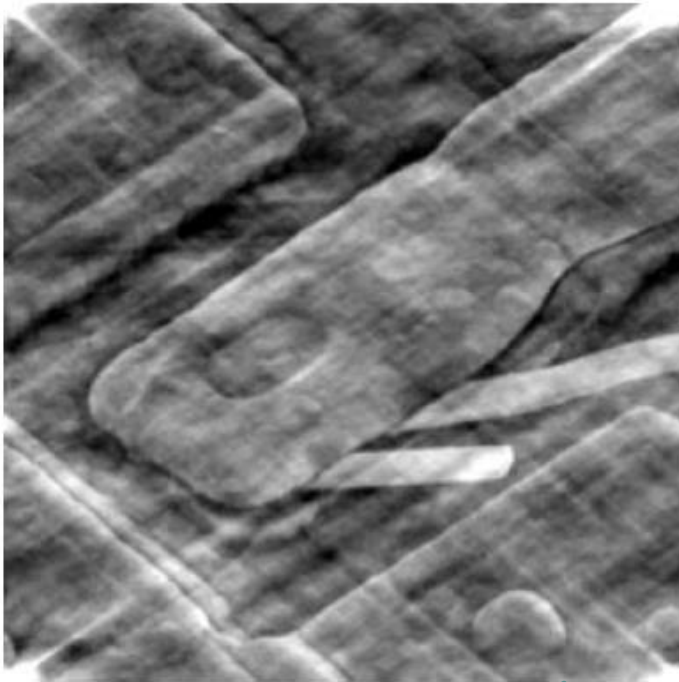
$$g(x, y) = \mathfrak{T}^{-1} [H(u, v) R(u, v) + jH(u, v) I(u, v)]$$

Filters affect the real and imaginary parts equally, and thus no effect on the phase.

These filters are called **zero-phase-shift** filters



Examples: Nonzero-Phase-Shift Filters



a b

FIGURE 4.35

(a) Image resulting from multiplying by 0.5 the phase angle in Eq. (4.6-15) and then computing the IDFT. (b) The result of multiplying the phase by 0.25. The spectrum was not changed in either of the two cases.

Even small
undesired

Phase angle
is multiplied
by 0.5

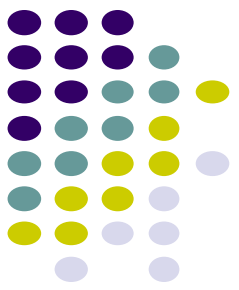
the phase angle can
the filtered output

Phase angle
is multiplied
by 0.25

usually

Summary:

Steps for Filtering in the Frequency Domain



1. Given an input image $f(x,y)$ of size $M \times N$, obtain the padding parameters P and Q , typically, $P = 2M$ and $Q = 2N$.
 2. Form a padded image, $f_p(x,y)$ of size $P \times Q$ by appending the necessary number of zeros to $f(x,y)$
 3. Multiply $f_p(x,y)$ by $(-1)^{x+y}$ to center its transform
 4. Compute the DFT, $F(u,v)$ of the image from step 3
 5. Generate a real, symmetric filter function*, $H(u,v)$, of size $P \times Q$ with center at coordinates $(P/2, Q/2)$
- *generate from a given spatial filter, we pad the spatial filter, multiply the expanded array by $(-1)^{x+y}$, and compute the DFT of the result to obtain a centered $H(u,v)$.

Summary:

Steps for Filtering in the Frequency Domain



6. Form the product $G(u, v) = H(u, v)F(u, v)$ using array multiplication
7. Obtain the processed image

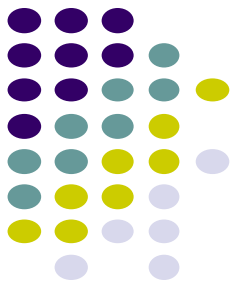
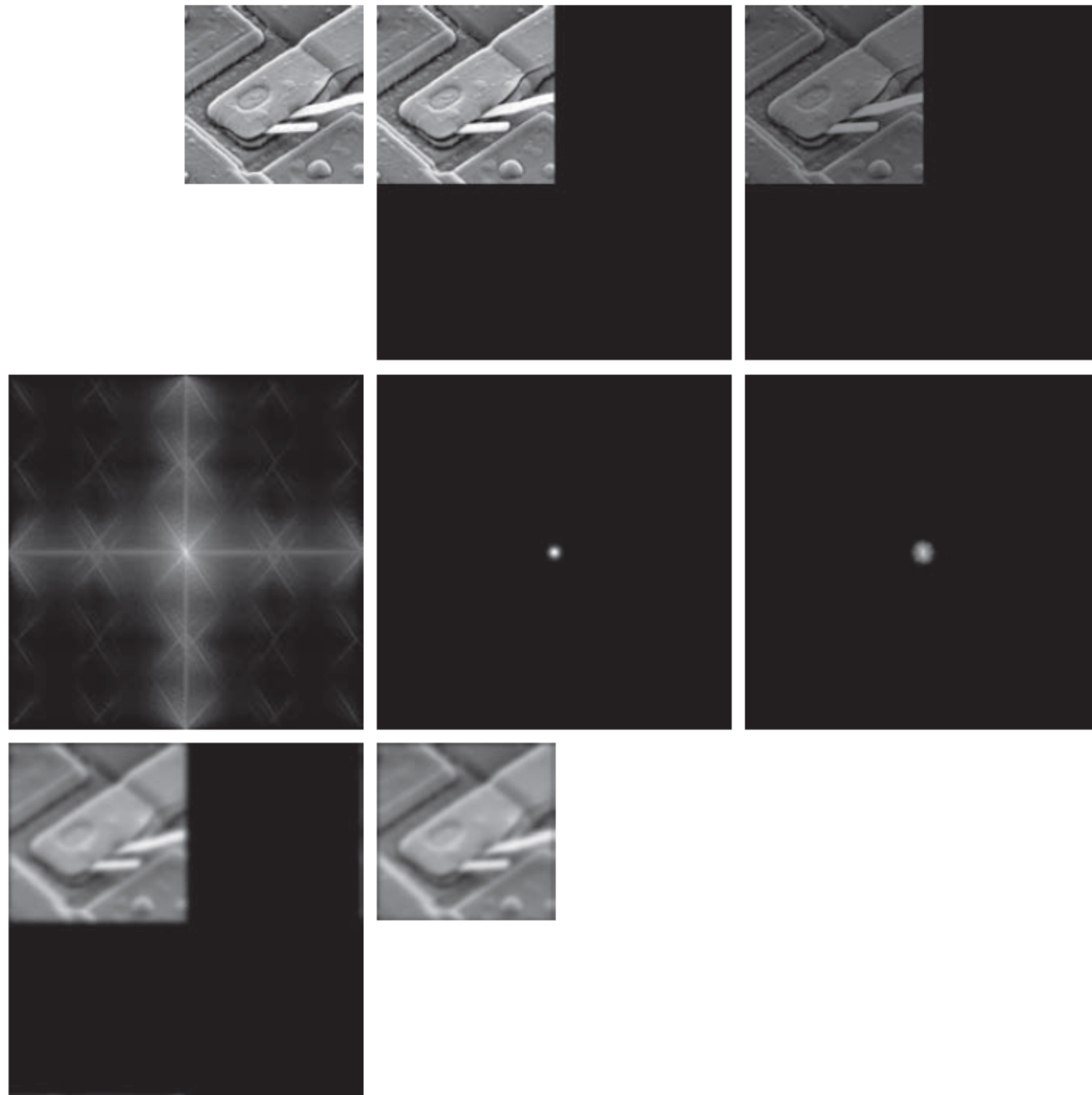
$$g_p(x, y) = \{real[\mathfrak{I}^{-1}[G(u, v)]]\}(-1)^{x+y}$$

8. Obtain the final processed result, $g(x, y)$, by extracting the $M \times N$ region from the top, left quadrant of $g_p(x, y)$

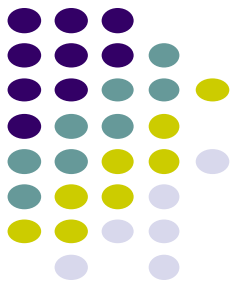
a	b	c
d	e	f
g	h	

FIGURE 4.35

- (a) An $M \times N$ image, f .
 (b) Padded image, f_p of size $P \times Q$.
 (c) Result of multiplying f_p by $(-1)^{x+y}$.
 (d) Spectrum of F . (e) Centered Gaussian lowpass filter transfer function, H , of size $P \times Q$.
 (f) Spectrum of the product HF .
 (g) Image g_p , the real part of the IDFT of HF , multiplied by $(-1)^{x+y}$.
 (h) Final result, g , obtained by extracting the first M rows and N columns of g_p .



Correspondence Between Filtering in the Spatial and Frequency Domains



Let $H(u)$ denote the 1-D frequency domain Gaussian filter

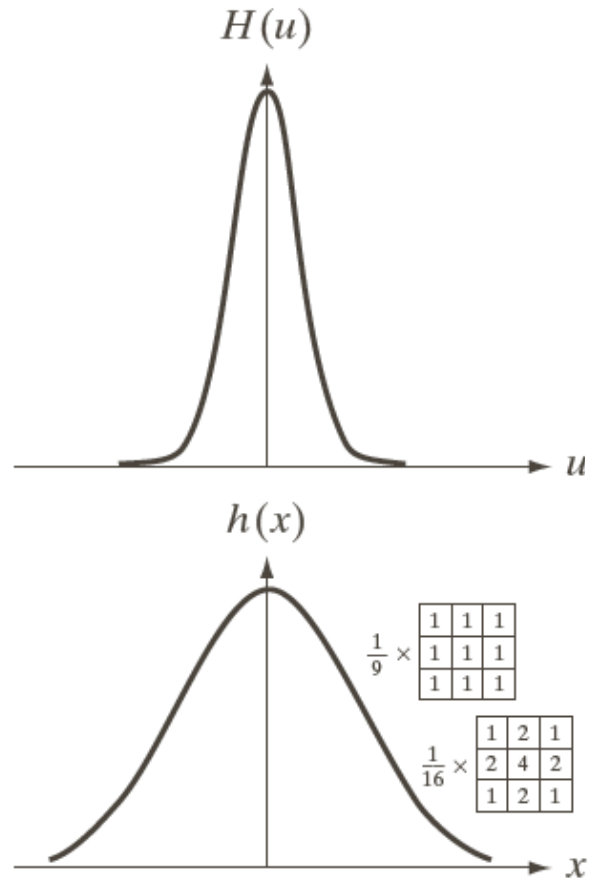
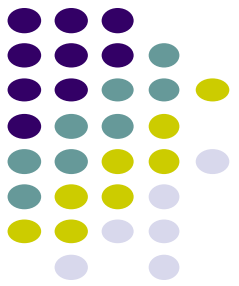
$$H(u) = Ae^{-u^2/2\sigma^2}$$

The corresponding filter in the spatial domain

$$h(x) = \sqrt{2\pi}\sigma Ae^{-2\pi^2\sigma^2x^2}$$

1. Both components are Gaussian and real
2. The functions behave reciprocally

Correspondence Between Filtering in the Spatial and Frequency Domains (contd.)



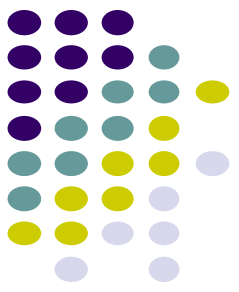
a
b

FIGURE 4.37

(a) A 1-D Gaussian lowpass filter in the frequency domain.

(b) Spatial lowpass filter corresponding to (a). (c) Gaussian

Correspondence Between Filtering in the Spatial and Frequency Domains (contd.)



Let $H(u)$ denote the difference of Gaussian filter

$$H(u) = Ae^{-u^2/2\sigma_1^2} - Be^{-u^2/2\sigma_2^2}$$

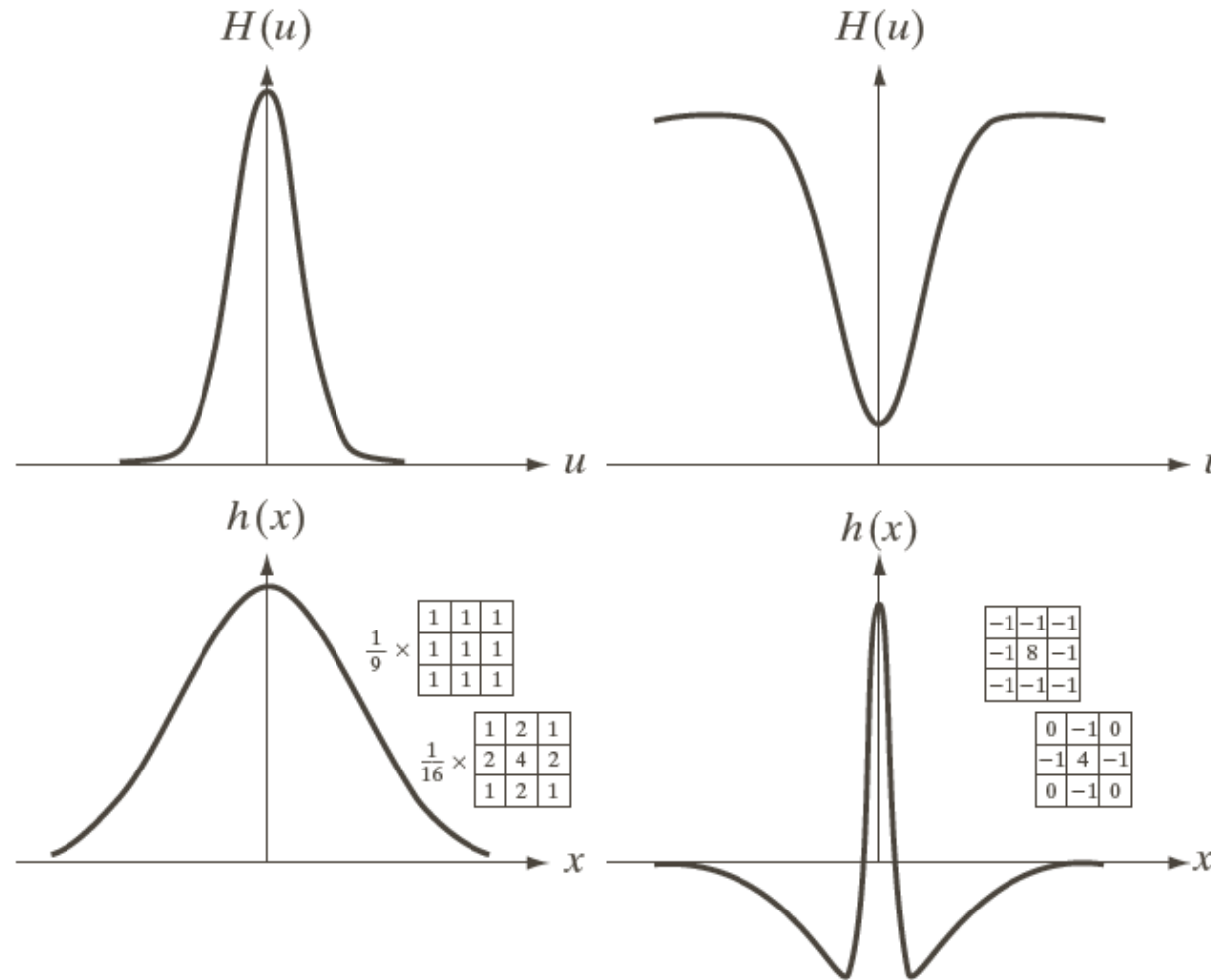
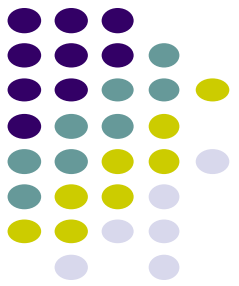
with $A \geq B$ and $\sigma_1 \geq \sigma_2$

The corresponding filter in the spatial domain

$$h(x) = \sqrt{2\pi}\sigma_1 Ae^{-2\pi^2\sigma_1^2 x^2} - \sqrt{2\pi}\sigma_2 Be^{-2\pi^2\sigma_2^2 x^2}$$

High-pass filter or low-pass filter ?

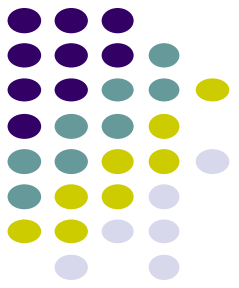
Correspondence Between Filtering in the Spatial and Frequency Domains (contd.)



a c
b d

FIGURE 4.37
(a) A 1-D Gaussian lowpass filter in the frequency domain. (b) Spatial lowpass filter corresponding to (a). (c) Gaussian highpass filter in the frequency domain. (d) Spatial highpass filter corresponding to (c). The small 2-D masks shown are spatial filters we used in Chapter 3.

Correspondence Between Filtering in the Spatial and Frequency Domains (contd.)



a b

FIGURE 4.37

(a) Image of a building, and
(b) its Fourier spectrum.



a	b
c	d

FIGURE 4.38

(a) A spatial kernel and perspective plot of its corresponding frequency domain filter transfer function.

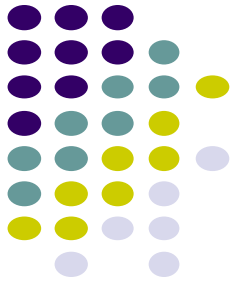
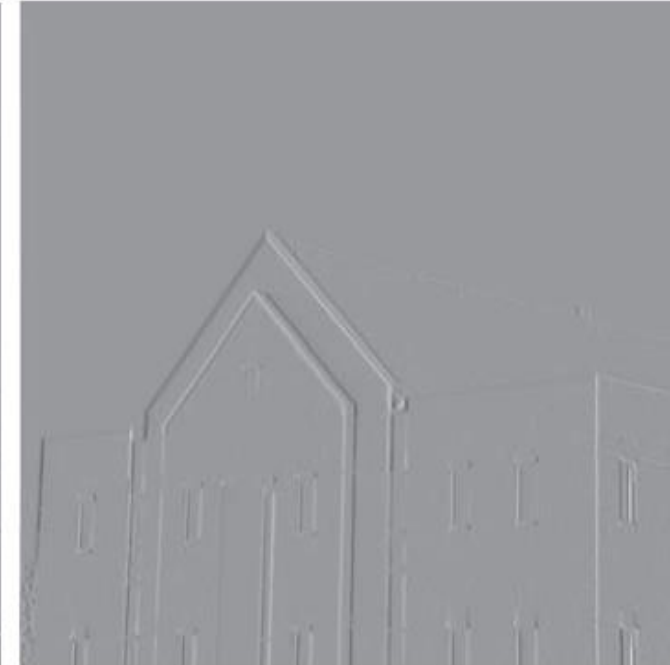
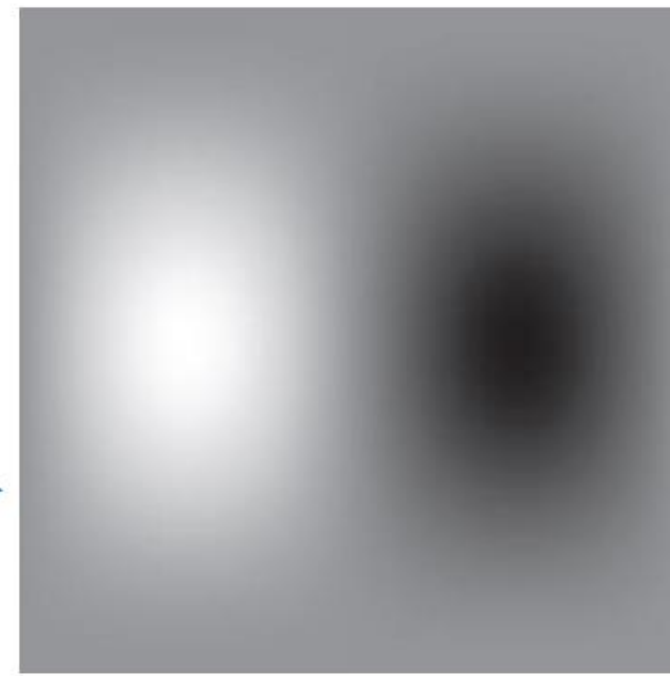
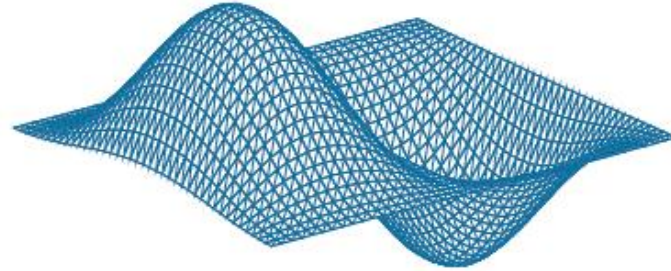
(b) Transfer function shown as an image.

(c) Result of filtering

Fig. 4.37(a) in the frequency domain with the transfer function in (b).

(d) Result of filtering the same image in the spatial domain with the kernel in (a). The results are identical.

-1	0	1
-2	0	2
-1	0	1





Ideal Low Pass Filters

Ideal Lowpass Filters (ILPF)

$$H(u, v) = \begin{cases} 1 & \text{if } D(u, v) \leq D_0 \\ 0 & \text{if } D(u, v) > D_0 \end{cases}$$

D_0 is a positive constant called cutoff frequency

$D(u, v)$ is the distance between a point (u, v) in the frequency domain and the center of the frequency rectangle

$$D(u, v) = [(u - P/2)^2 + (v - Q/2)^2]^{1/2}$$

Standard cutoff frequency loci

$$P_T = \sum_{u=0}^{P-1} \sum_{v=0}^{Q-1} P(u, v)$$

Ideal Low Pass Filters (contd.)

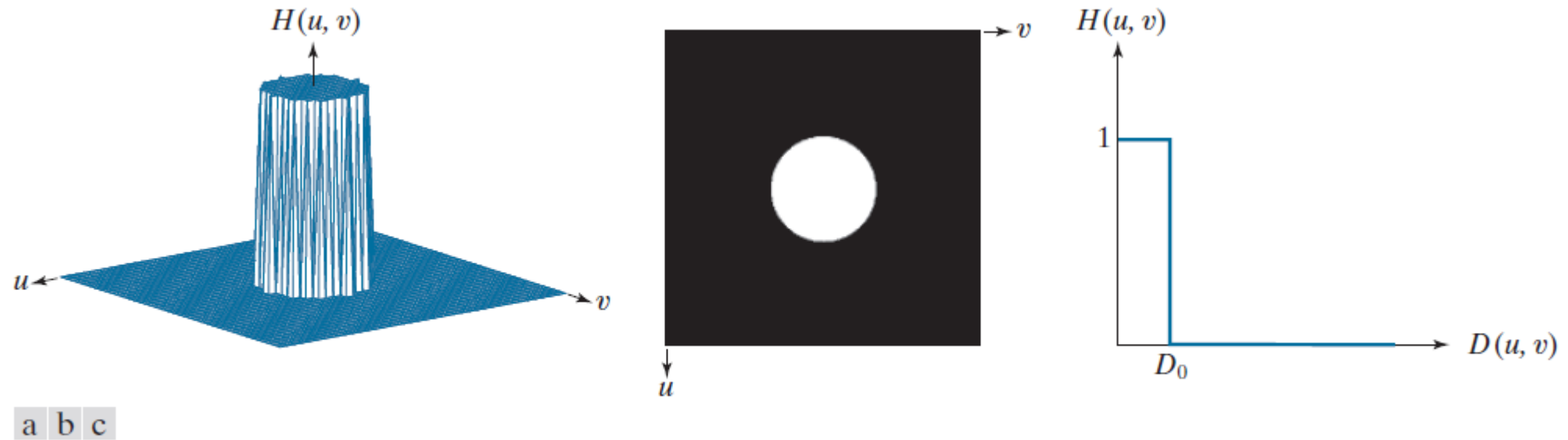
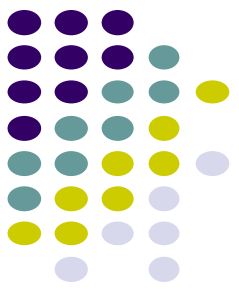
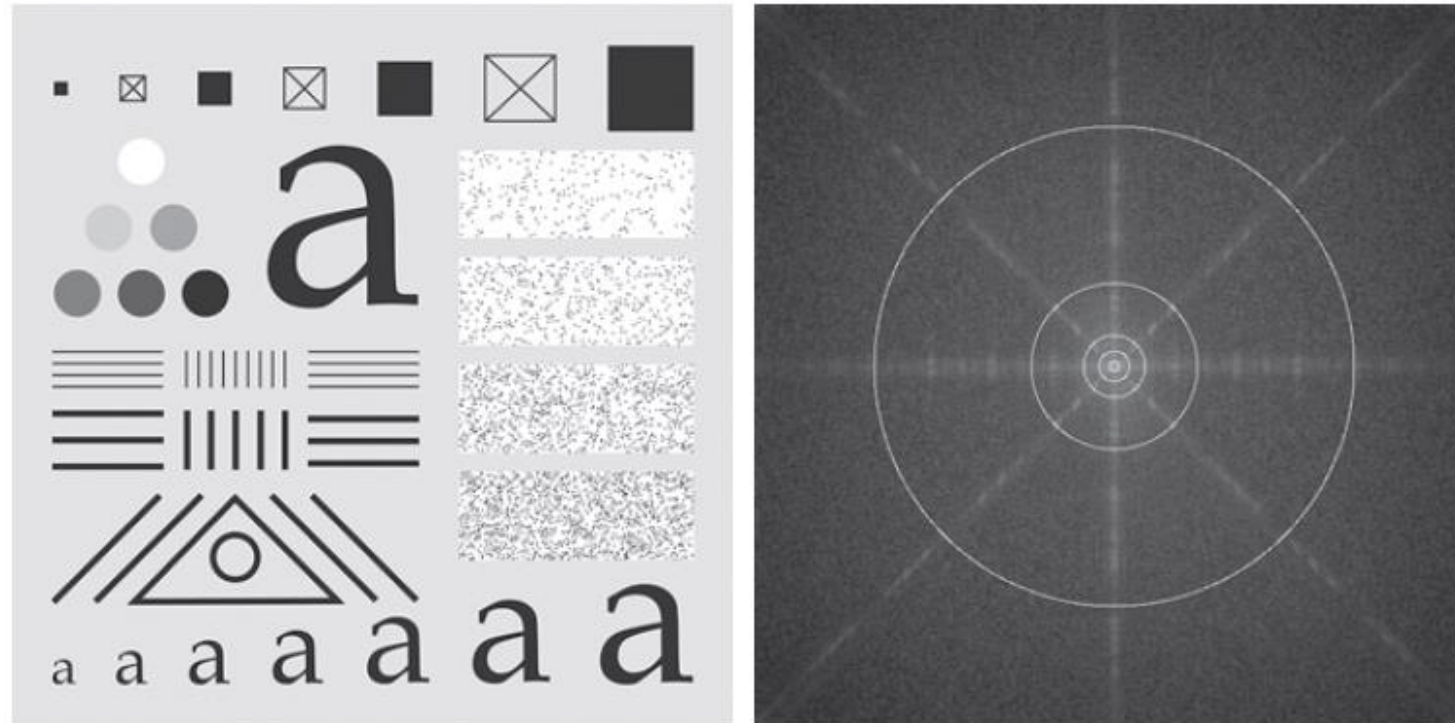


FIGURE 4.39 (a) Perspective plot of an ideal lowpass-filter transfer function. (b) Function displayed as an image. (c) Radial cross section.

Ideal Low Pass Filters (contd.)



a b

FIGURE 4.40 (a) Test pattern of size 688×688 pixels, and (b) its spectrum. The spectrum is double the image size as a result of padding, but is shown half size to fit. The circles have radii of 10, 30, 60, 160, and 460 pixels with respect to the full-size spectrum. The radii enclose 86.9, 92.8, 95.1, 97.6, and 99.4% of the padded image power, respectively.

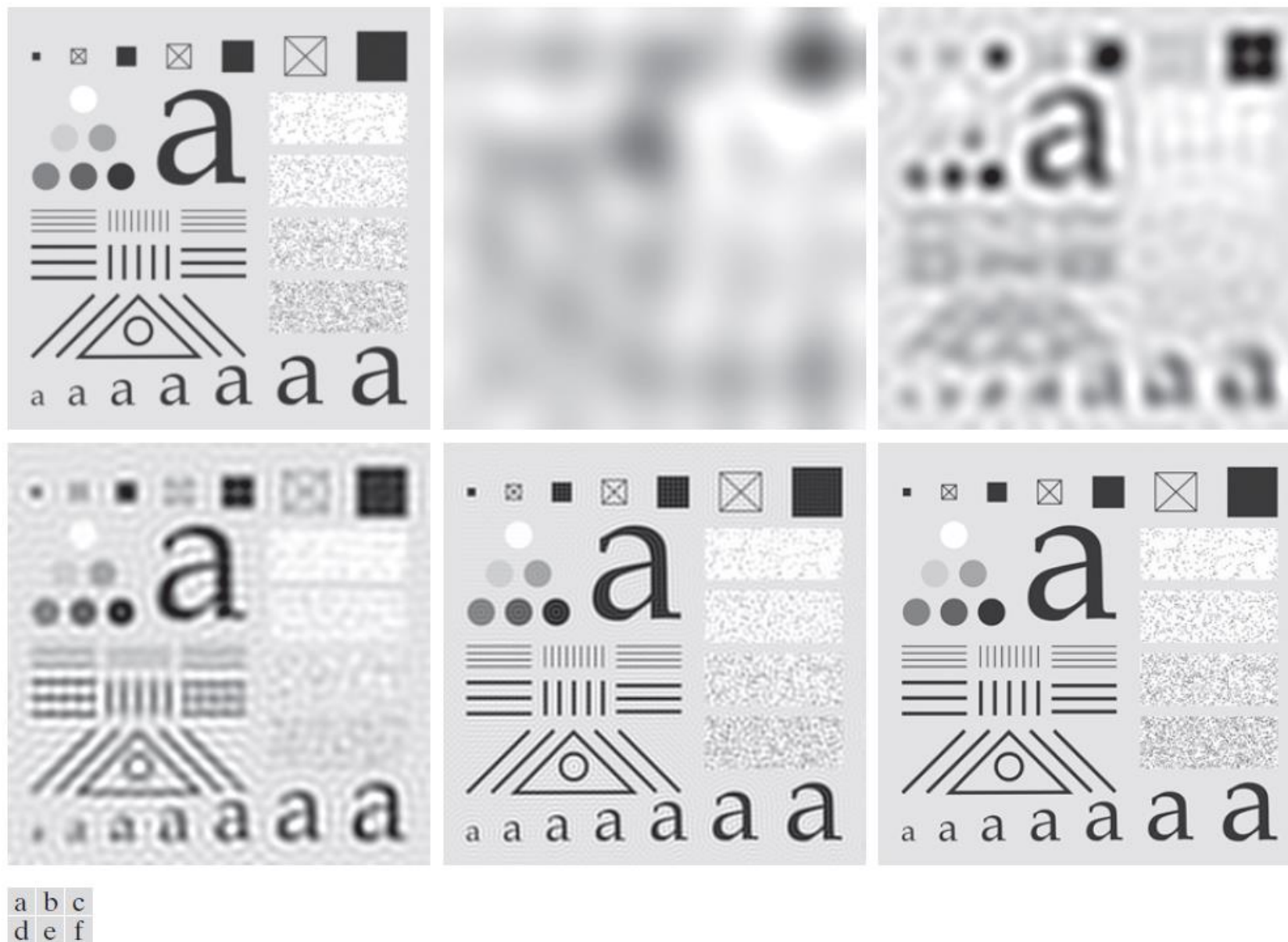
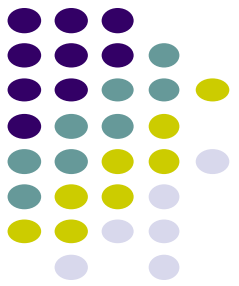
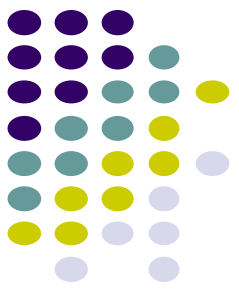


FIGURE 4.41 (a) Original image of size 688×688 pixels. (b)–(f) Results of filtering using ILPFs with cutoff frequencies set at radii values 10, 30, 60, 160, and 460, as shown in Fig. 4.40(b). The power removed by these filters was 13.1, 7.2, 4.9, 2.4, and 0.6% of the total, respectively. We used mirror padding to avoid the black borders characteristic of zero padding, as illustrated in Fig. 4.31(c).

Ideal Low Pass Filters (contd.)



a b c

FIGURE 4.42

- (a) Frequency domain ILPF transfer function.
- (b) Corresponding spatial domain kernel function.
- (c) Intensity profile of a horizontal line through the center of (b).



Butterworth Low Pass Filters



Butterworth Lowpass Filters (BLPF) of order n and with cutoff frequency D_0

$$H(u, v) = \frac{1}{1 + [D(u, v) / D_0]^{2n}}$$

Butterworth Low Pass Filters (contd.)

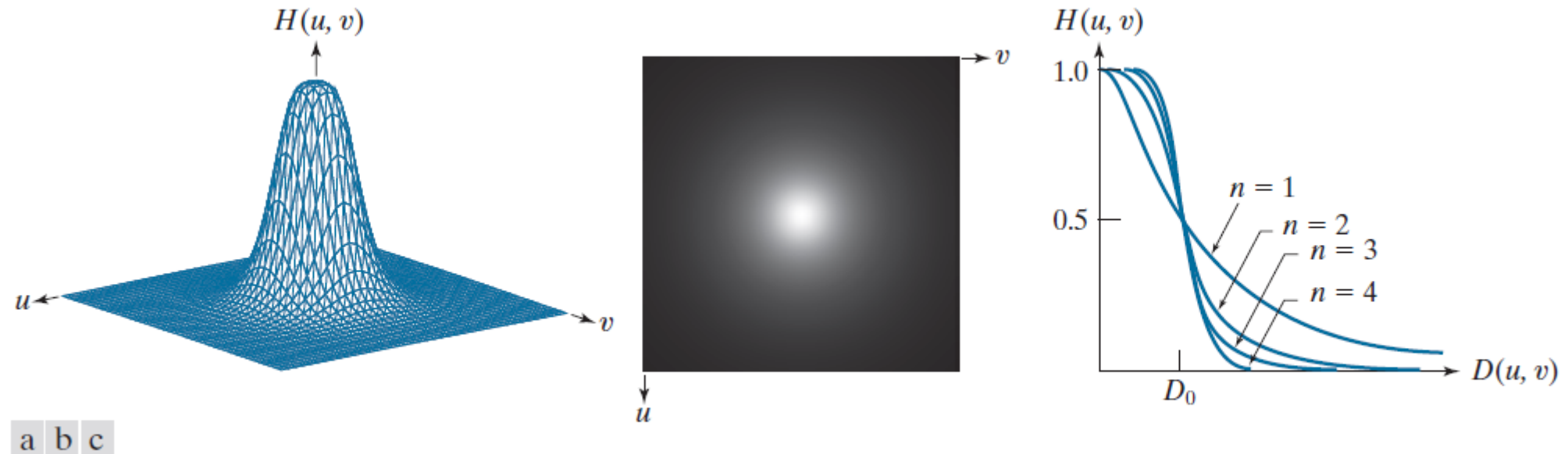


FIGURE 4.45 (a) Perspective plot of a Butterworth lowpass-filter transfer function. (b) Function displayed as an image. (c) Radial cross sections of BLPFs of orders 1 through 4.

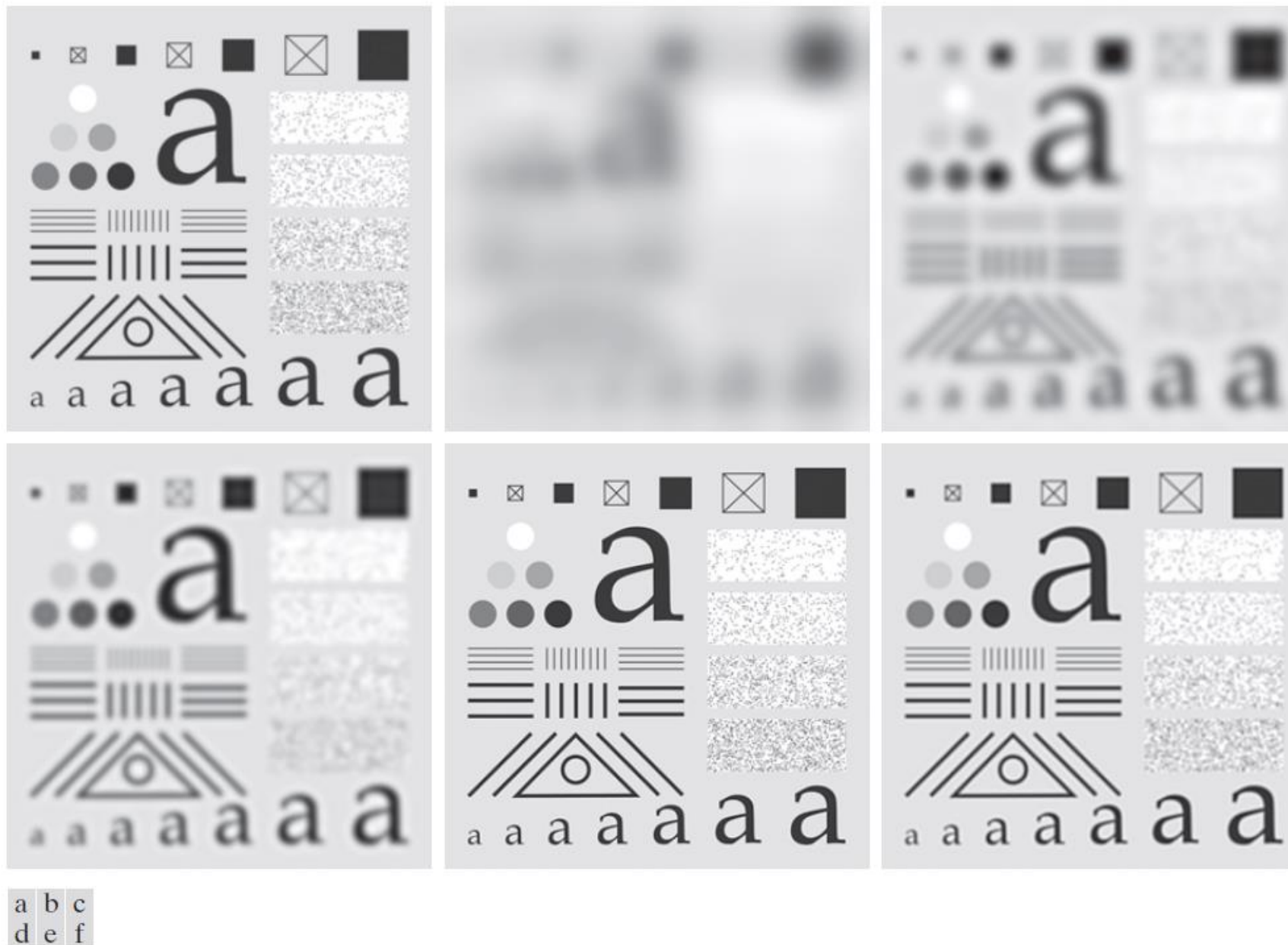
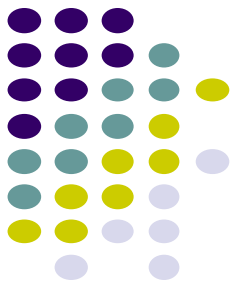
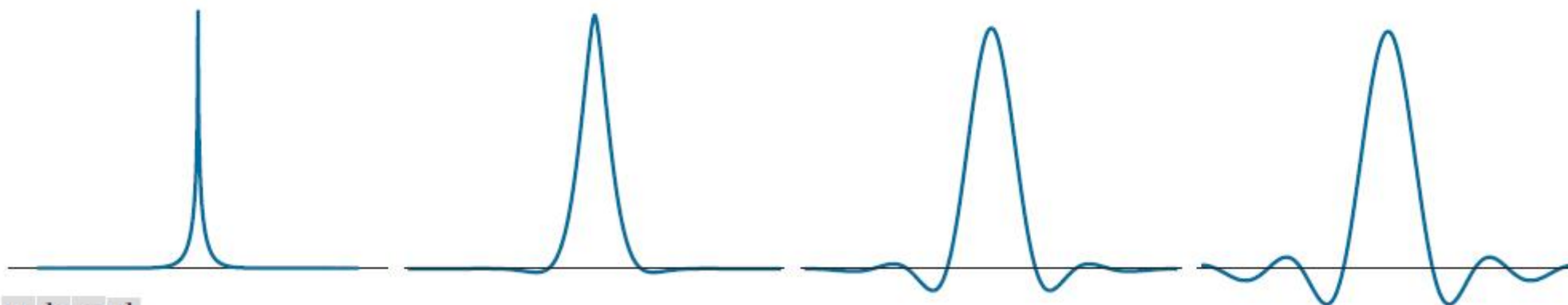
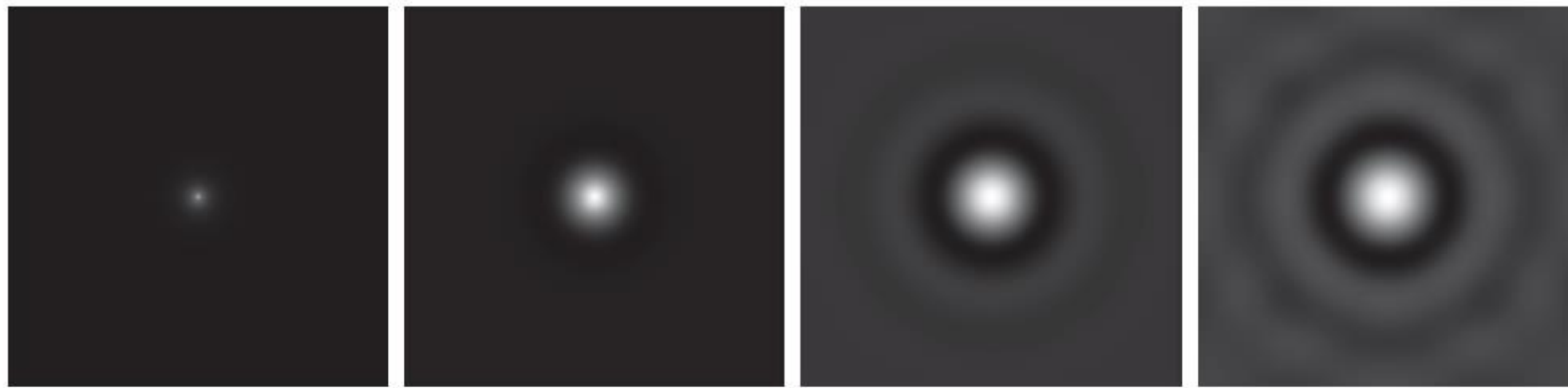


FIGURE 4.46 (a) Original image of size 688×688 pixels. (b)–(f) Results of filtering using BLPFs with cutoff frequencies at the radii shown in Fig. 4.40 and $n = 2.25$. Compare with Figs. 4.41 and 4.44. We used mirror padding to avoid the black borders characteristic of zero padding.



a	b	c	d
e	f	g	h

FIGURE 4.47 (a)–(d) Spatial representations (i.e., spatial kernels) corresponding to BLPF transfer functions of size 1000×1000 pixels, cut-off frequency of 5, and order 1, 2, 5, and 20, respectively. (e)–(h) Corresponding intensity profiles through the center of the filter functions.

Gaussian Low Pass Filters



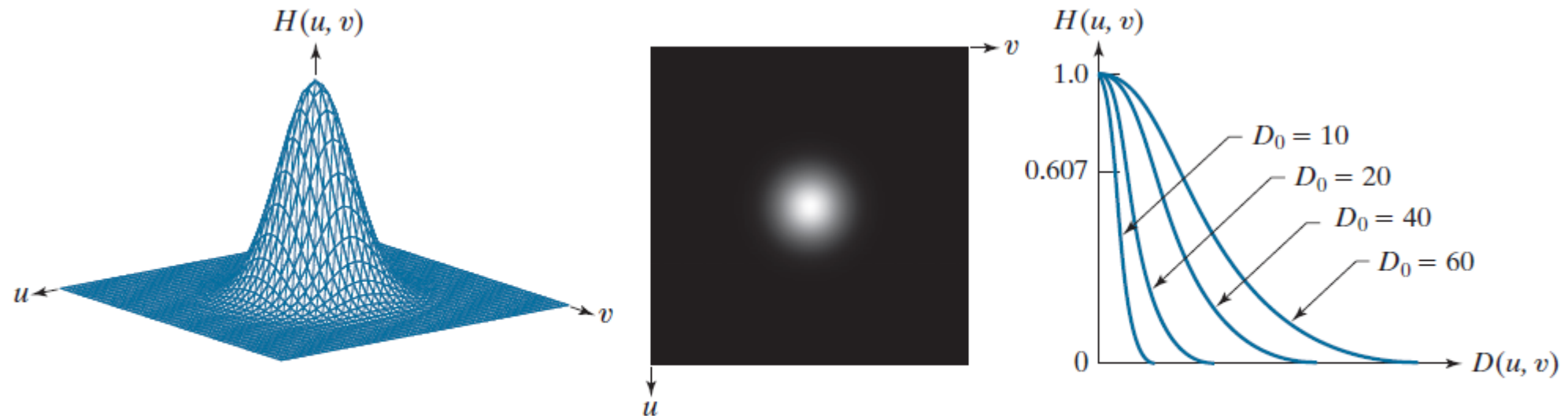
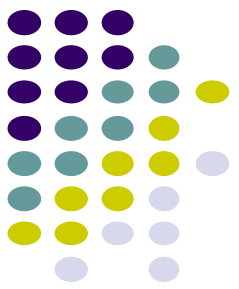
Gaussian Lowpass Filters (GLPF) in two dimensions is given

$$H(u, v) = e^{-D^2(u, v)/2\sigma^2}$$

By letting $\sigma = D_0$

$$H(u, v) = e^{-D^2(u, v)/2D_0^2}$$

Gaussian Low Pass Filters (contd.)



a b c

FIGURE 4.43 (a) Perspective plot of a GLPF transfer function. (b) Function displayed as an image. (c) Radial cross sections for various values of D_0 .

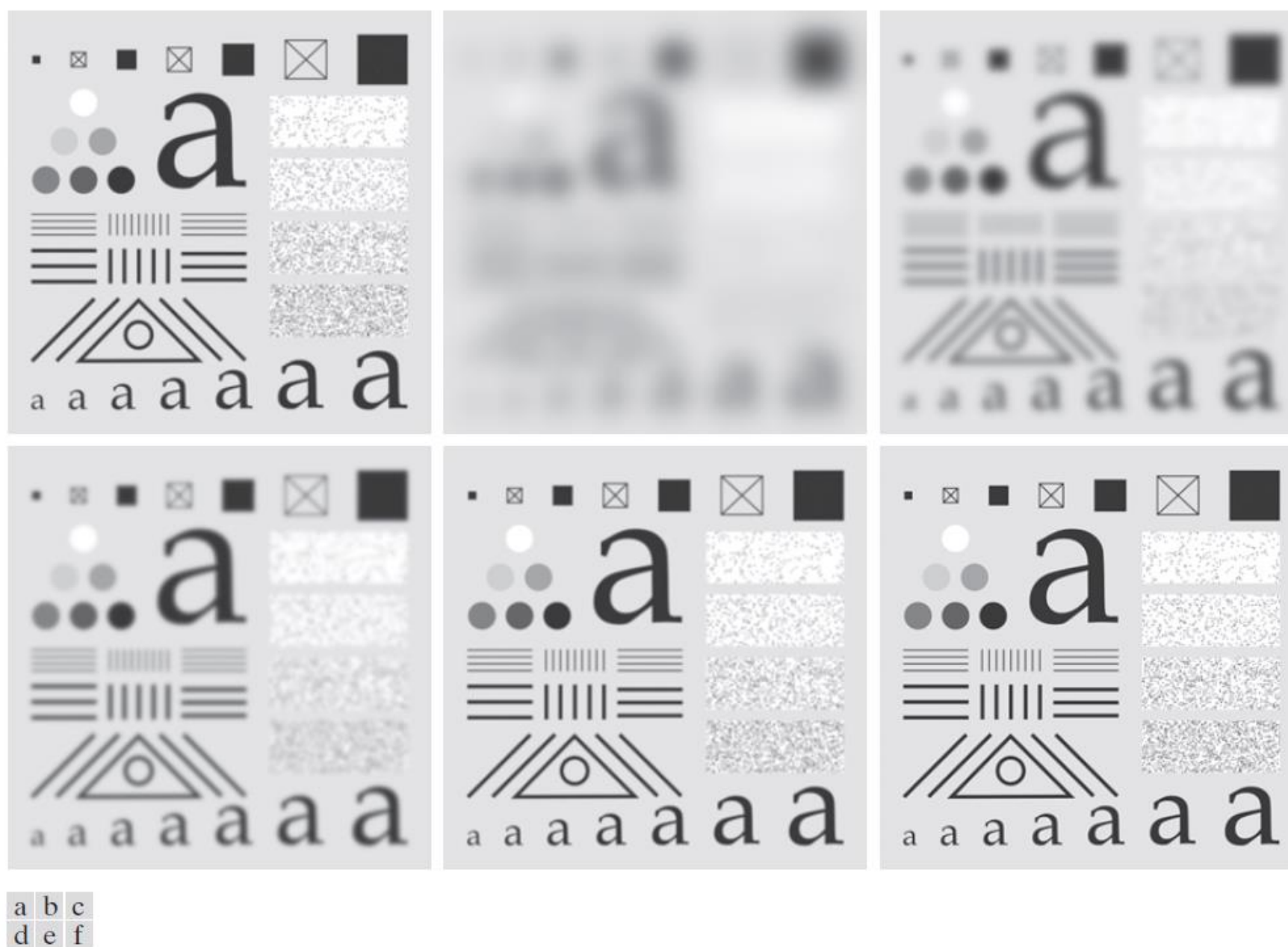
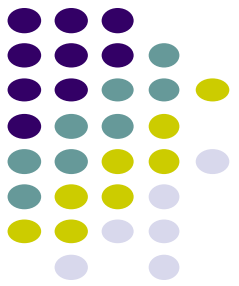
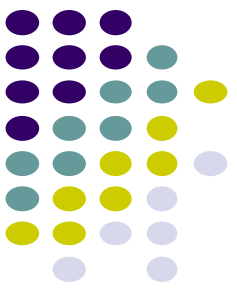


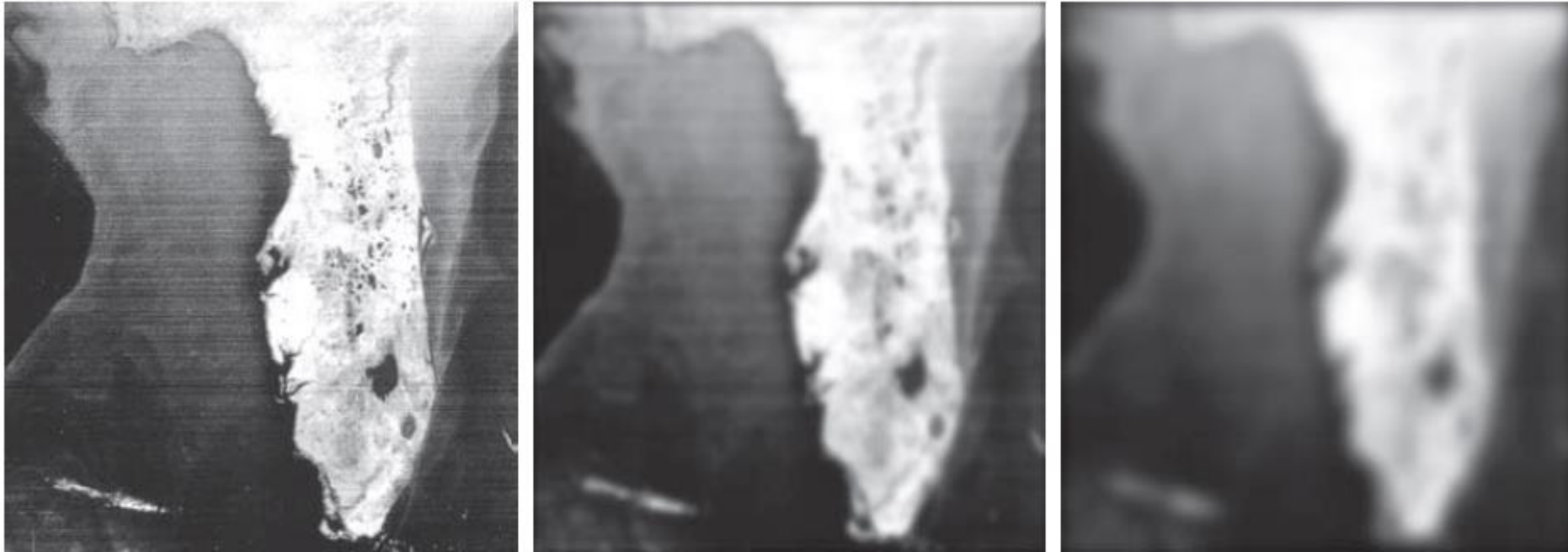
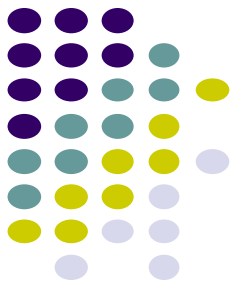
FIGURE 4.44 (a) Original image of size 688×688 pixels. (b)–(f) Results of filtering using GLPFs with cutoff frequencies at the radii shown in Fig. 4.40. Compare with Fig. 4.41. We used mirror padding to avoid the black borders characteristic of zero padding.



a b c

FIGURE 4.49 (a) Original 785×732 image. (b) Result of filtering using a GLPF with $D_0 = 150$. (c) Result of filtering using a GLPF with $D_0 = 130$. Note the reduction in fine skin lines in the magnified sections in (b) and (c).

Gaussian Low Pass Filters (contd.)



a b c

FIGURE 4.50 (a) 808×754 satellite image showing prominent horizontal scan lines. (b) Result of filtering using a GLPF with $D_0 = 50$. (c) Result of using a GLPF with $D_0 = 20$. (Original image courtesy of NOAA.)



Sharpening in the Frequency Domain

- Edges and fine detail in images are associated with high frequency components
- *High pass filters* – only pass the high frequencies, drop the low ones
- High pass frequencies are precisely the reverse of low pass filters, so:

$$H_{hp}(u, v) = 1 - H_{lp}(u, v)$$



Ideal High Pass Filters

- The ideal high pass filter is given by:

$$H(u, v) = \begin{cases} 0 & \text{if } D(u, v) \leq D_0 \\ 1 & \text{if } D(u, v) > D_0 \end{cases}$$

- D_0 is the cut-off distance as before.



Butterworth High Pass Filters

- The Butterworth high pass filter is given as:

$$H(u, v) = \frac{1}{1 + [D_0 / D(u, v)]^{2n}}$$

- n is the order and D_0 is the cut off distance as before.



Gaussian High Pass Filters

- The Gaussian high pass filter is given as:

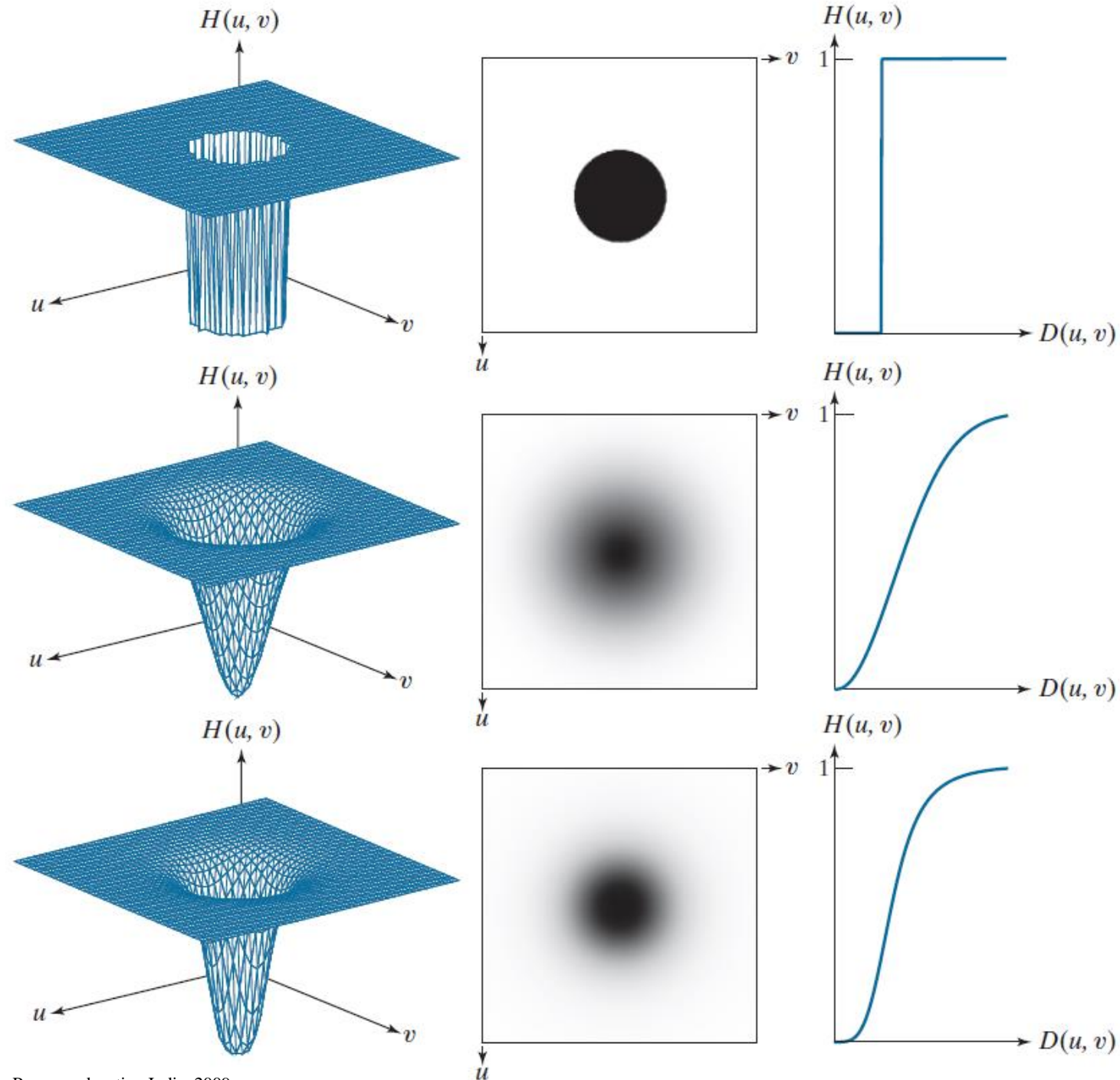
$$H(u, v) = 1 - e^{-D^2(u, v) / 2D_0^2}$$

- D_0 is the cut off distance as before.

a	b	c
d	e	f
g	h	i

FIGURE 4.51

Top row:
Perspective plot,
image, and, radial
cross section of
an IHPF transfer
function. Middle
and bottom
rows: The same
sequence for
GHPF and BHPF
transfer functions.
(The thin image
borders were
added for clarity.
They are not part
of the data.)



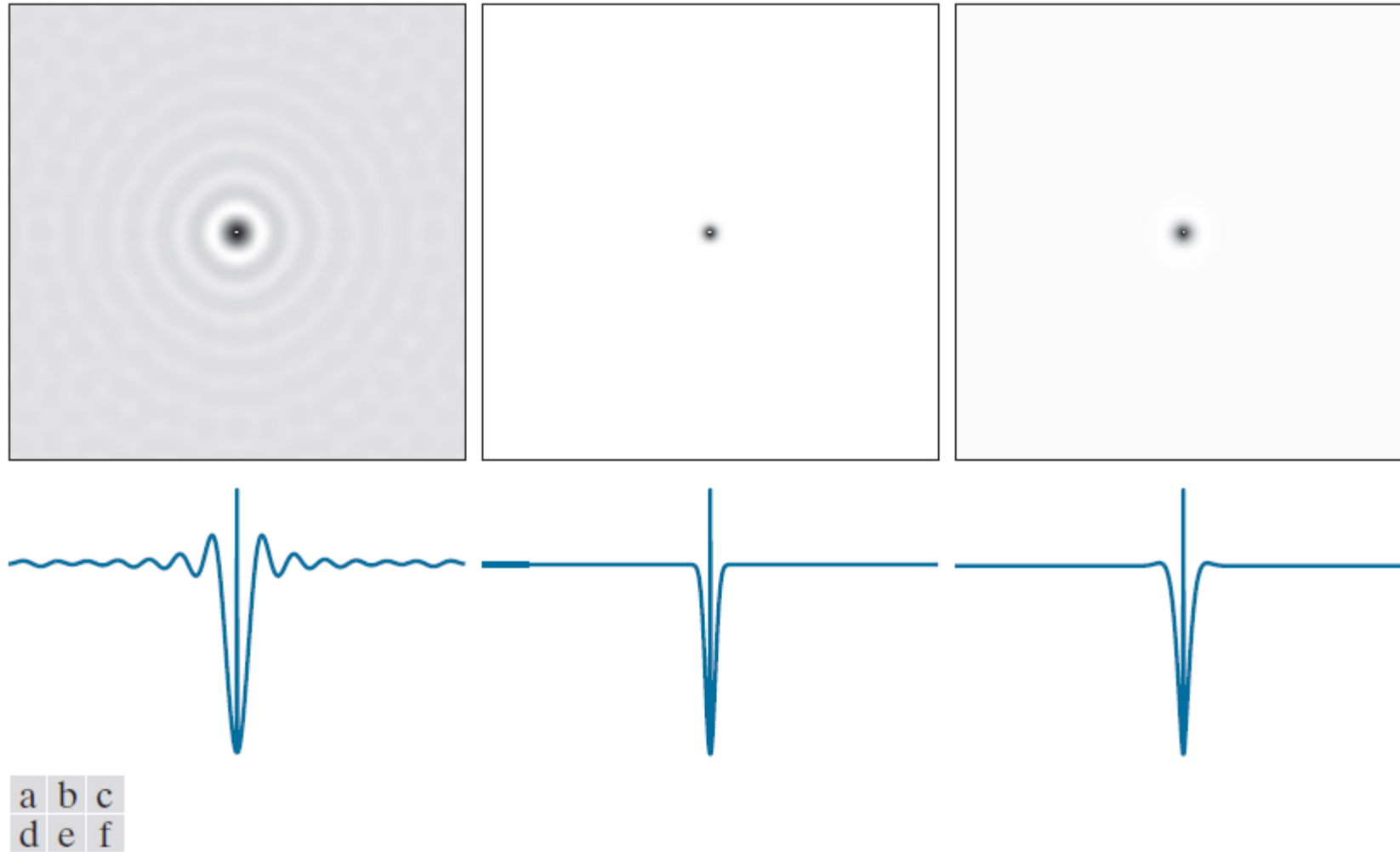


FIGURE 4.52 (a)–(c): Ideal, Gaussian, and Butterworth highpass spatial kernels obtained from IHPPF, GHPF, and BHPF frequency-domain transfer functions. (The thin image borders are not part of the data.) (d)–(f): Horizontal intensity profiles through the centers of the kernels.

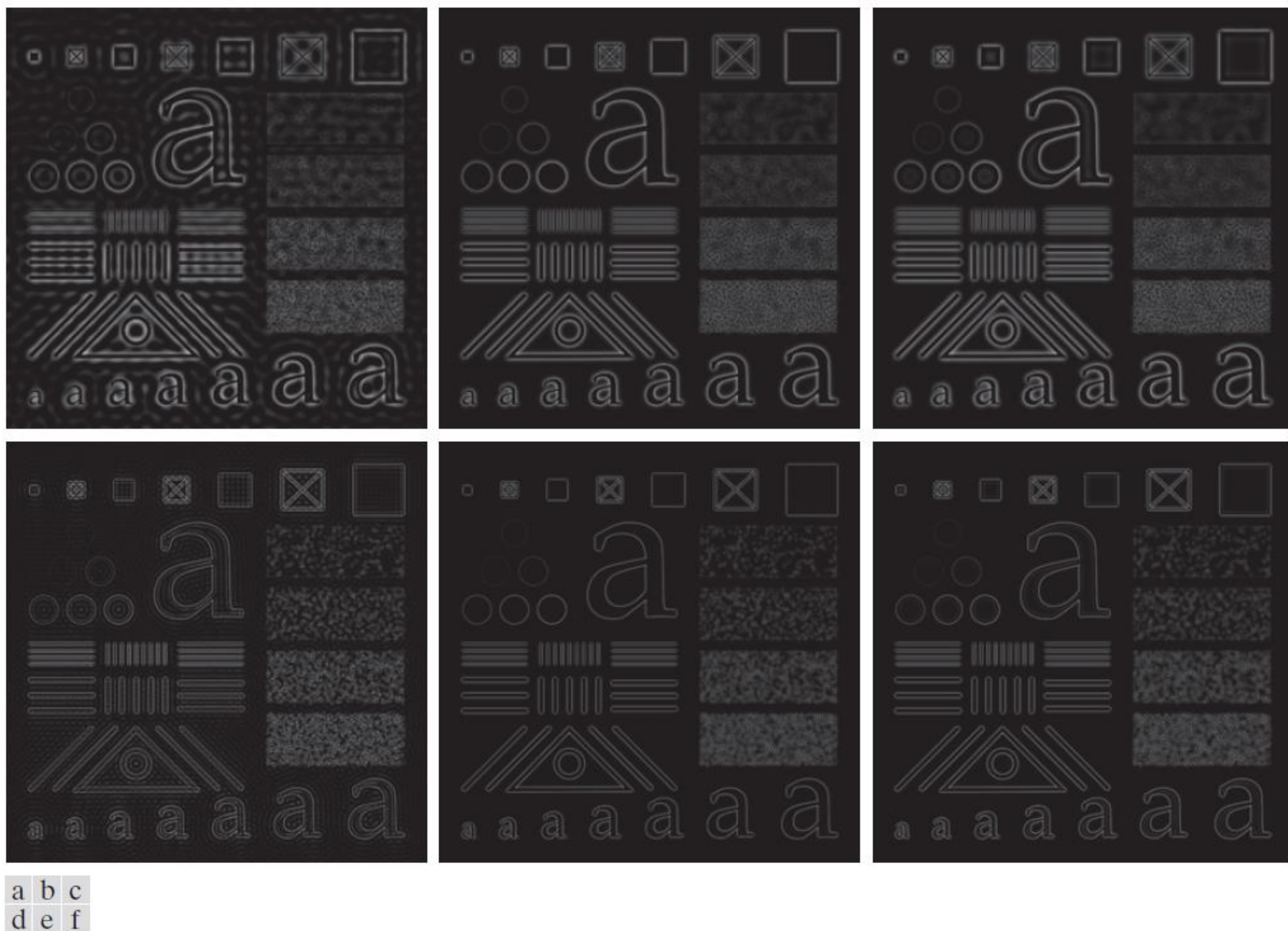
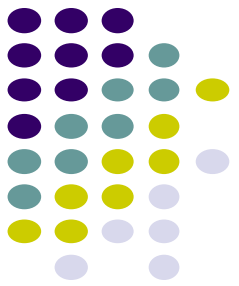


FIGURE 4.53 Top row: The image from Fig. 4.40(a) filtered with IHPF, GHPF, and BHPF transfer functions using $D_0 = 60$ in all cases ($n = 2$ for the BHPF). Second row: Same sequence, but using $D_0 = 160$.



The Laplacian in the Frequency Domain

$$H(u, v) = -4\pi^2(u^2 + v^2)$$

$$\begin{aligned} H(u, v) &= -4\pi^2 \left[(u - P/2)^2 + (v - Q/2)^2 \right] \\ &= -4\pi^2 D^2(u, v) \end{aligned}$$

The Laplacian image

$$\nabla^2 f(x, y) = \mathfrak{F}^{-1} \{ H(u, v) F(u, v) \}$$

Enhancement is obtained

$$g(x, y) = f(x, y) + c \nabla^2 f(x, y) \quad c = -1$$

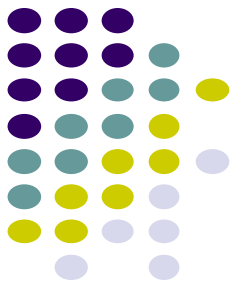
The Laplacian in the Frequency Domain (contd.)



The enhanced image

$$\begin{aligned} g(x, y) &= \mathfrak{F}^{-1} \{ F(u, v) - H(u, v)F(u, v) \} \\ &= \mathfrak{F}^{-1} \{ [1 - H(u, v)] F(u, v) \} \\ &= \mathfrak{F}^{-1} \{ [1 + 4\pi^2 D^2(u, v)] F(u, v) \} \end{aligned}$$

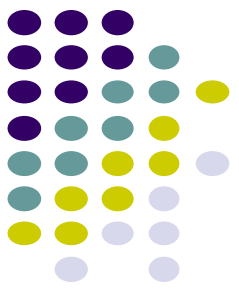
The Laplacian in the Frequency Domain (contd.)



a b

FIGURE 4.58
(a) Original, blurry image.
(b) Image enhanced using the Laplacian in the frequency domain. Compare with Fig. 3.38(e).

Unsharp Masking, Highboost Filtering and High-Frequency-Emphasis Filtering



$$g_{mask}(x, y) = f(x, y) - f_{LP}(x, y)$$

$$f_{LP}(x, y) = \mathfrak{F}^{-1} [H_{LP}(u, v)F(u, v)]$$

Unsharp masking and highboost filtering

$$g(x, y) = f(x, y) + k * g_{mask}(x, y)$$

$$\begin{aligned} g(x, y) &= \mathfrak{F}^{-1} \left\{ \left[1 + k * [1 - H_{LP}(u, v)] \right] F(u, v) \right\} \\ &= \mathfrak{F}^{-1} \left\{ [1 + k * H_{HP}(u, v)] F(u, v) \right\} \end{aligned}$$

Unsharp Masking, Highboost Filtering and High-Frequency-Emphasis Filtering (contd.)



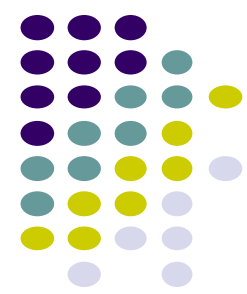
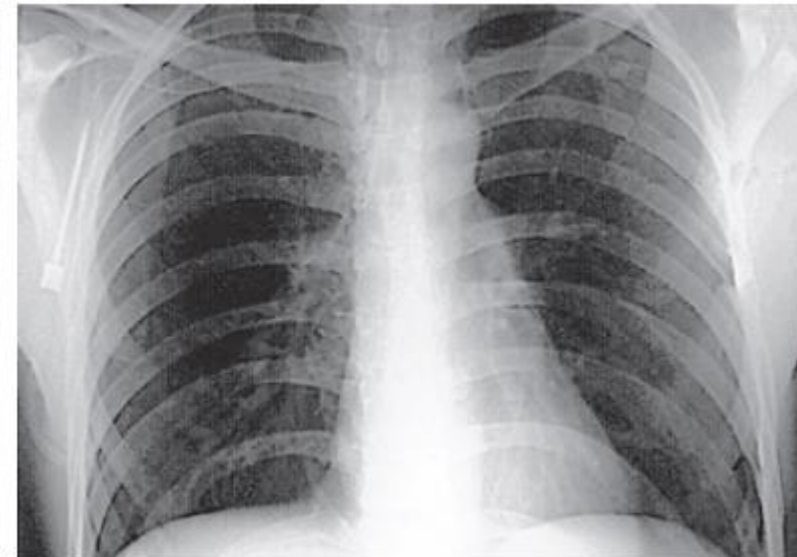
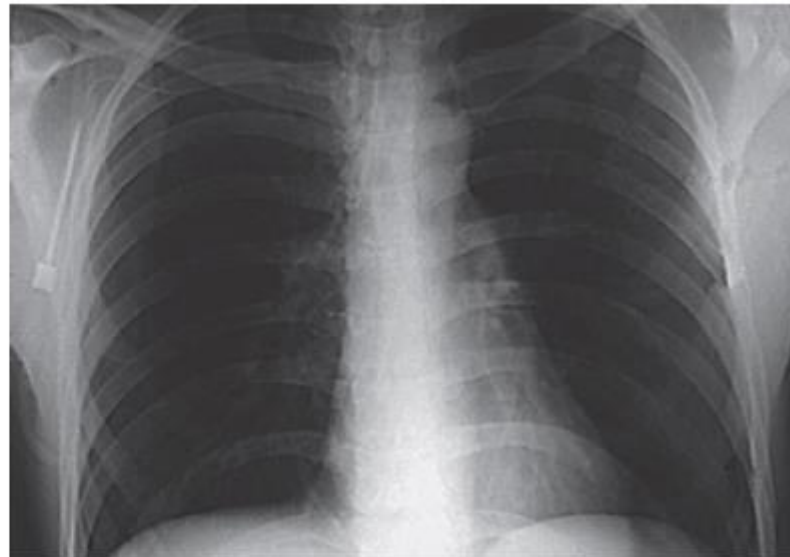
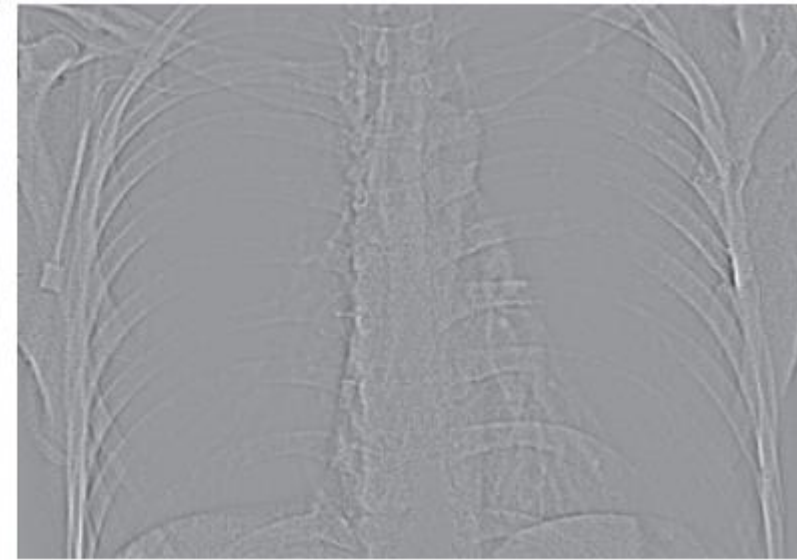
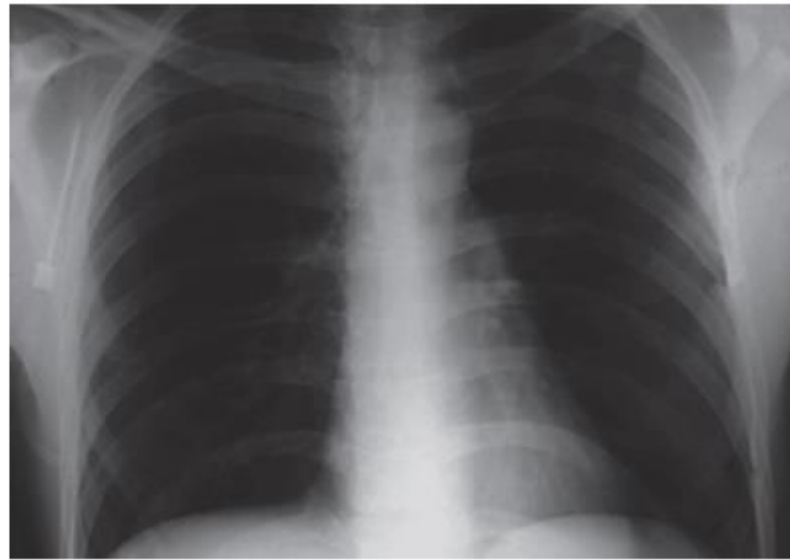
$$g(x, y) = \mathfrak{F}^{-1} \left\{ \left[k_1 + k_2 * H_{HP}(u, v) \right] F(u, v) \right\}$$

$$k_1 \geq 0 \quad \text{and} \quad k_2 \geq 0$$

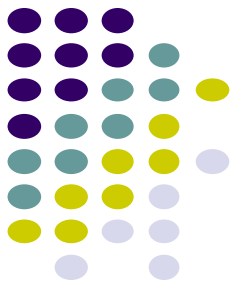
a	b
c	d

FIGURE 4.57

(a) A chest X-ray.
 (b) Result of filtering with a GHPF function.
 (c) Result of high-frequency-emphasis filtering using the same GHPF.
 (d) Result of performing histogram equalization on (c).
 (Original image courtesy of Dr. Thomas R. Gest, Division of Anatomical Sciences, University of Michigan Medical School.)



Homomorphic Filtering



$$f(x, y) = i(x, y)r(x, y)$$

$$\mathfrak{I}[f(x, y)] \neq \mathfrak{I}[i(x, y)]\mathfrak{I}[r(x, y)]$$

$$z(x, y) = \ln f(x, y) = \ln i(x, y) + \ln r(x, y)$$

$$\mathfrak{I}\{z(x, y)\} = \mathfrak{I}\{\ln f(x, y)\} = \mathfrak{I}\{\ln i(x, y)\} + \mathfrak{I}\{\ln r(x, y)\}$$

$$Z(u, v) = F_i(u, v) + F_r(u, v)$$

Homomorphic Filtering (contd.)



$$\begin{aligned} S(u, v) &= H(u, v)Z(u, v) \\ &= H(u, v)F_i(u, v) + H(u, v)F_r(u, v) \end{aligned}$$

$$\begin{aligned} s(x, y) &= \mathfrak{F}^{-1} \{ S(u, v) \} \\ &= \mathfrak{F}^{-1} \{ H(u, v)F_i(u, v) + H(u, v)F_r(u, v) \} \\ &= \mathfrak{F}^{-1} \{ H(u, v)F_i(u, v) \} + \mathfrak{F}^{-1} \{ H(u, v)F_r(u, v) \} \\ &= i'(x, y) + r'(x, y) \end{aligned}$$

$$g(x, y) = e^{s(x, y)} = e^{i'(x, y)} e^{r'(x, y)} = i_0(x, y) r_0(x, y)$$

Homomorphic Filtering (contd.)

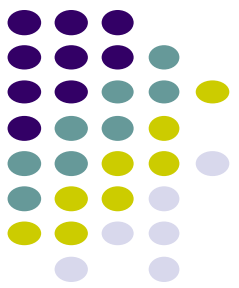
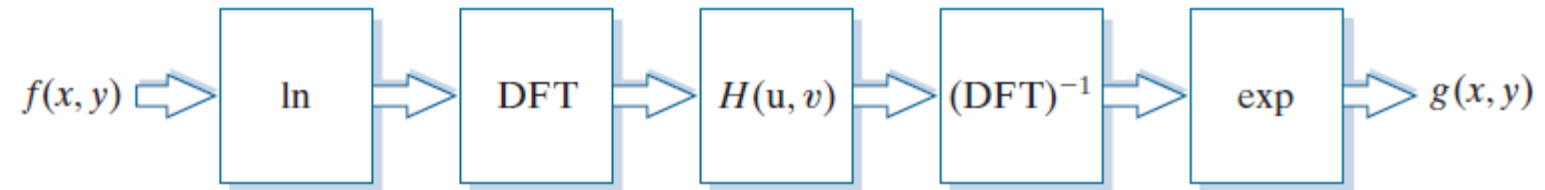


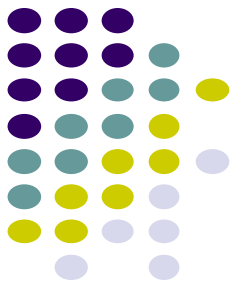
FIGURE 4.58

Summary of steps
in homomorphic
filtering.



- The illumination component of an image generally is characterized by slow spatial variations, while the reflectance component tends to vary abruptly.
- These characteristics lead to associating the low frequencies of the Fourier transform of the logarithm of an image with illumination the high frequencies with reflectance.

Homomorphic Filtering (contd.)



$$H(u, v) = (\gamma_H - \gamma_L) \left[1 - e^{-c \left[D^2(u, v) / D_0^2 \right]} \right] + \gamma_L$$

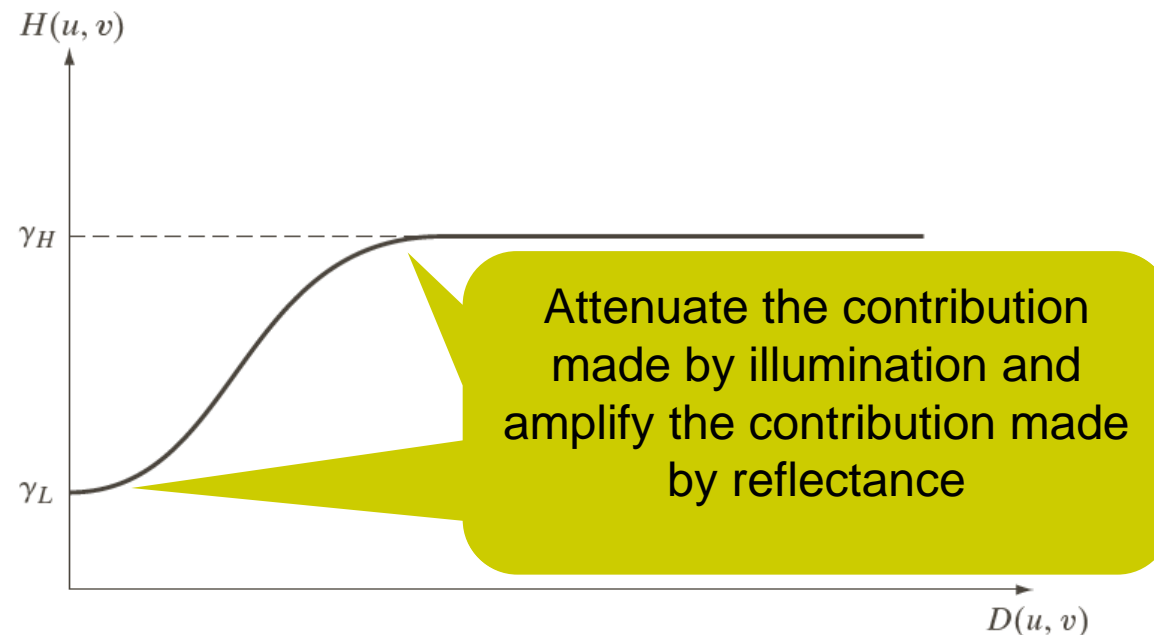


FIGURE 4.61
Radial cross section of a circularly symmetric homomorphic filter function. The vertical axis is at the center of the frequency rectangle and $D(u, v)$ is the distance from the center.

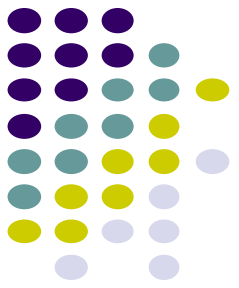


$$\gamma_L = 0.25$$

$$\gamma_H = 2$$

$$c = 1$$

$$D_0 = 80$$



a b

FIGURE 4.62
 (a) Full body PET scan. (b) Image enhanced using homomorphic filtering. (Original image courtesy of Dr. Michael E. Casey, CTI PET Systems.)



Selective Filtering

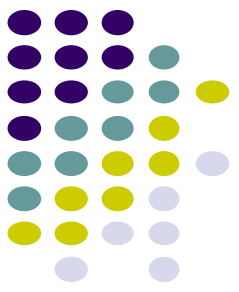
- **Non-Selective Filters:**

- operate over the entire frequency rectangle

- **Selective Filters**

- operate over some part, not entire frequency rectangle
 - **bandreject or bandpass:** process specific bands
 - **notch filters:** process small regions of the frequency rectangle

Key requirements for bandpass transfer function



- Value of function
 - should be $[0,1]$
 - Zero at a distance C_0 from the origin
- Able to specify a value for W

Selective Filtering: Bandreject and Bandpass Filters

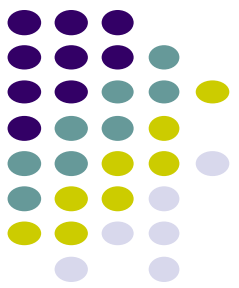


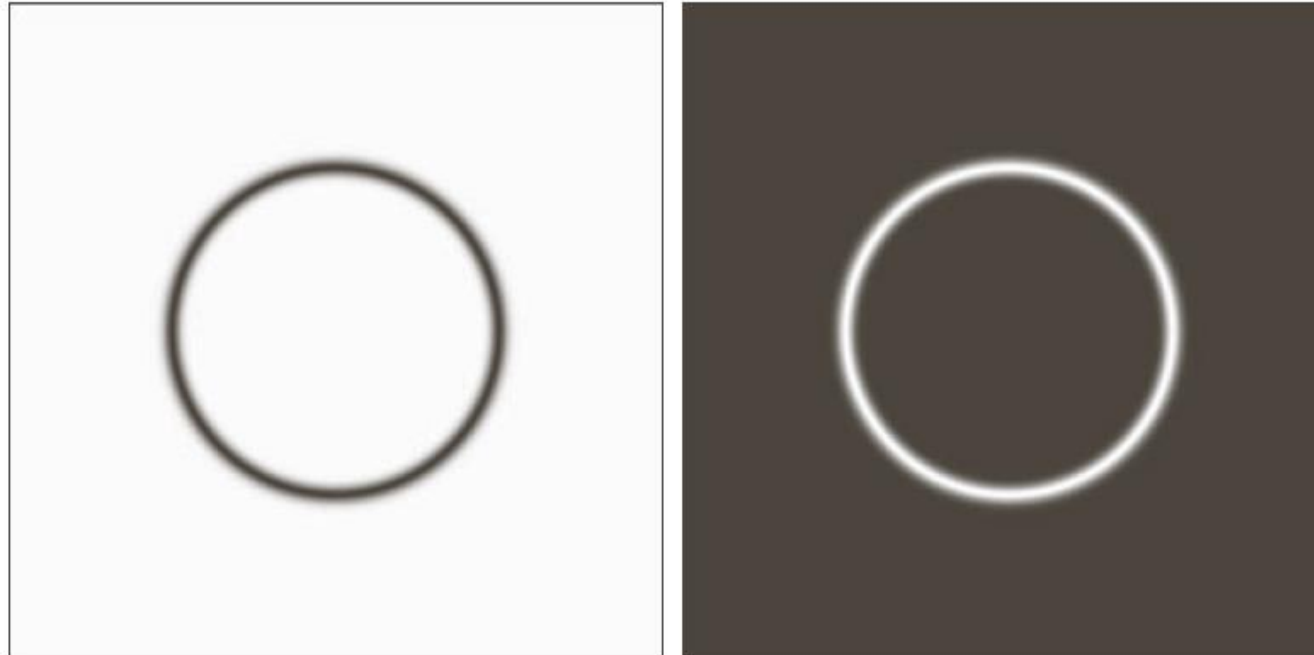
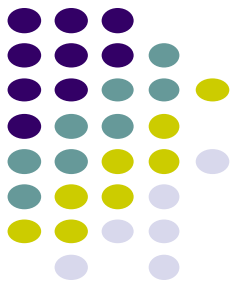
TABLE 4.6

Bandreject filters. W is the width of the band, D is the distance $D(u, v)$ from the center of the filter, D_0 is the cutoff frequency, and n is the order of the Butterworth filter. We show D instead of $D(u, v)$ to simplify the notation in the table.

Ideal	Butterworth	Gaussian
$H(u, v) = \begin{cases} 0 & \text{if } D_0 - \frac{W}{2} \leq D \leq D_0 + \frac{W}{2} \\ 1 & \text{otherwise} \end{cases}$	$H(u, v) = \frac{1}{1 + \left[\frac{DW}{D^2 - D_0^2} \right]^{2n}}$	$H(u, v) = 1 - e^{-\left[\frac{D^2 - D_0^2}{DW} \right]^2}$

$$H_{BP}(u, v) = 1 - H_{BR}(u, v)$$

Selective Filtering: Bandreject and Bandpass Filters (contd.)



a b

FIGURE 4.63

(a) Bandreject
Gaussian filter.
(b) Corresponding
bandpass filter.
The thin black
border in (a) was
added for clarity; it
is not part of the
data.



Selective Filtering: Notch Filters

- Zero-phase-shift filters must be symmetric about the origin.
- A notch with center at (u_0, v_0) must have a corresponding notch at location $(-u_0, -v_0)$.
- Notch reject filters are constructed as products of highpass filters whose centers have been translated to the centers of the notches.

$$H_{NR}(u, v) = \prod_{k=1}^Q H_k(u, v) H_{-k}(u, v)$$

where $H_k(u, v)$ and $H_{-k}(u, v)$ are highpass filters whose centers are at (u_k, v_k) and $(-u_k, -v_k)$, respectively.



Selective Filtering: Notch Filters (contd.)

$$H_{NR}(u, v) = \prod_{k=1}^Q H_k(u, v) H_{-k}(u, v)$$

where $H_k(u, v)$ and $H_{-k}(u, v)$ are highpass filters whose centers are at (u_k, v_k) and $(-u_k, -v_k)$, respectively.

A Butterworth notch reject filter of order n

$$H_{NR}(u, v) = \prod_{k=1}^3 \left[\frac{1}{1 + [D_{0k} / D_k(u, v)]^{2n}} \right] \left[\frac{1}{1 + [D_{0k} / D_{-k}(u, v)]^{2n}} \right]$$

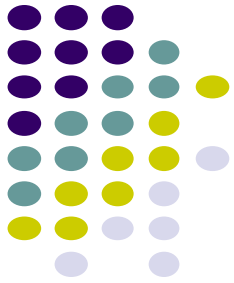
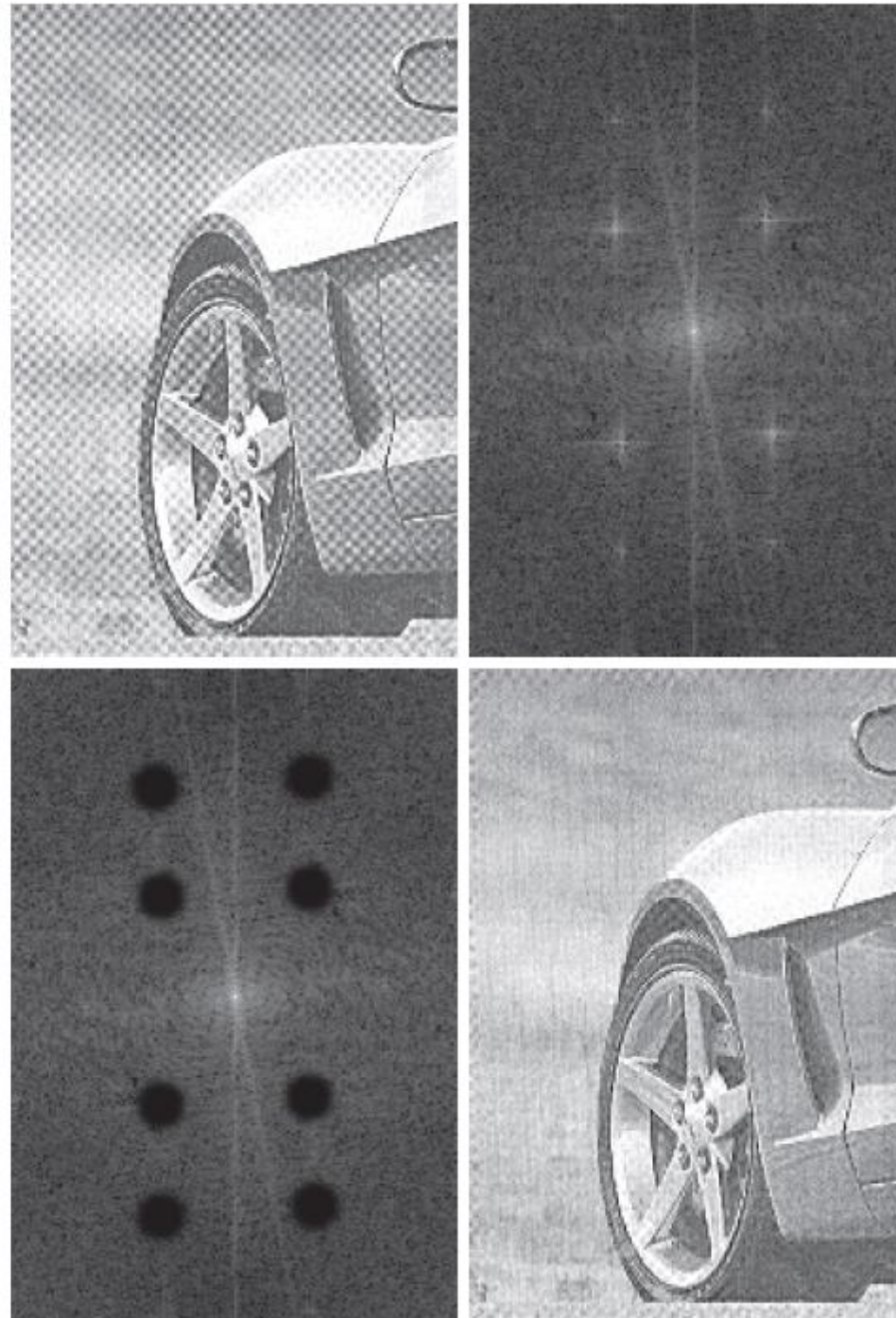
$$D_k(u, v) = \left[(u - M / 2 - u_k)^2 + (v - N / 2 - v_k)^2 \right]^{1/2}$$

$$D_{-k}(u, v) = \left[(u - M / 2 + u_k)^2 + (v - N / 2 + v_k)^2 \right]^{1/2}$$

a	b
c	d

FIGURE 4.64

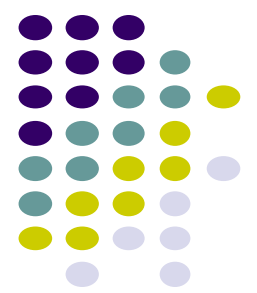
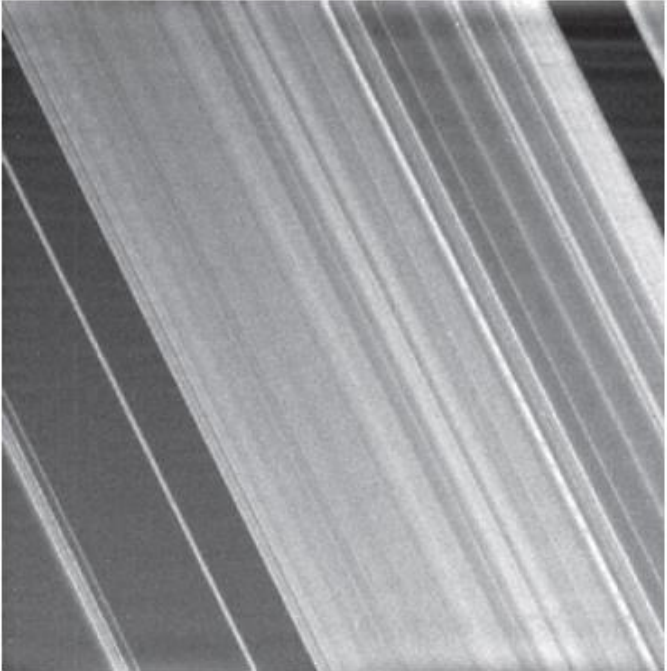
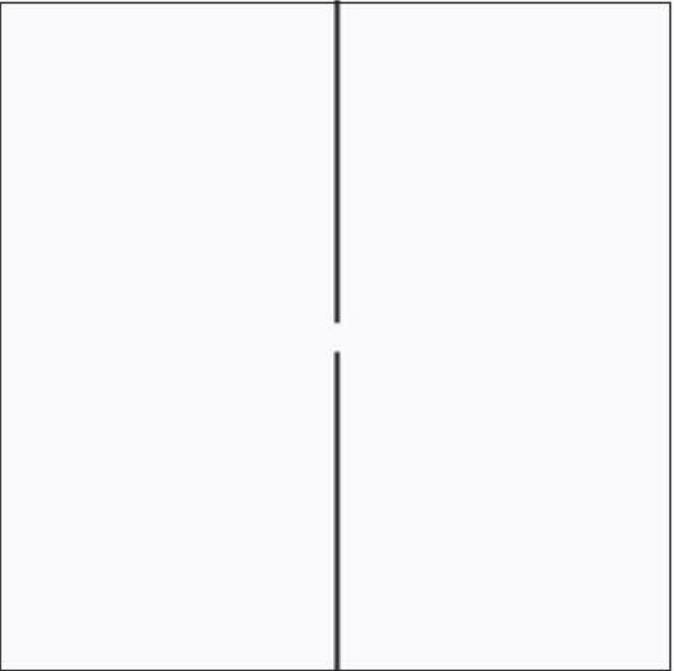
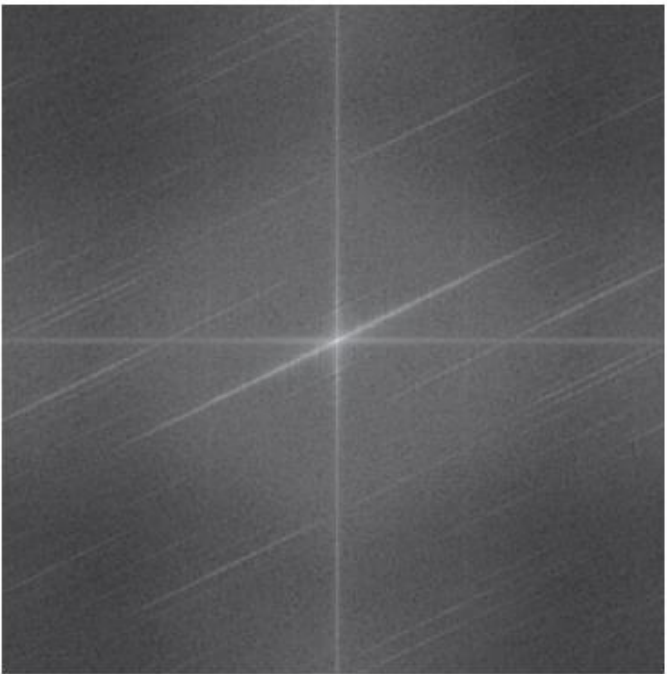
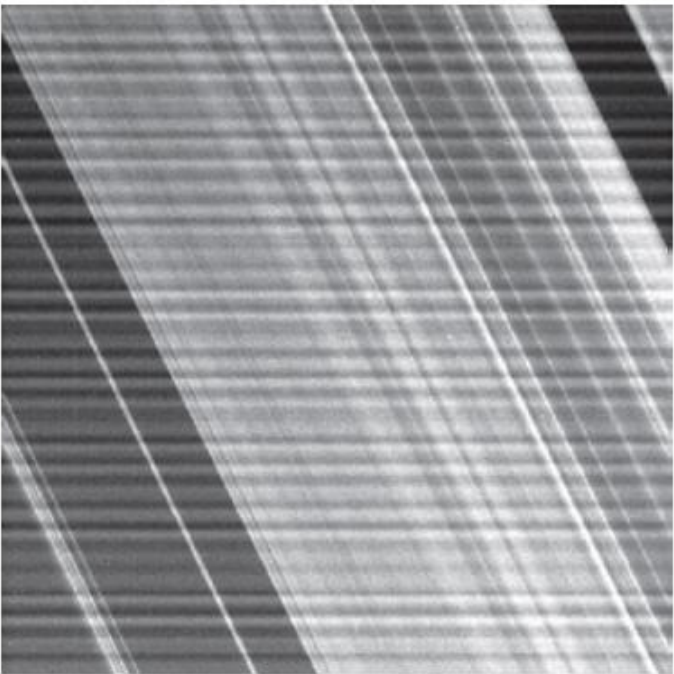
(a) Sampled newspaper image showing a moiré pattern.
 (b) Spectrum.
 (c) Fourier transform multiplied by a Butterworth notch reject filter transfer function.
 (d) Filtered image.



a	b
c	d

FIGURE 4.65

(a) Image of Saturn rings showing nearly periodic interference.
 (b) Spectrum.
 (The bursts of energy in the vertical axis near the origin correspond to the interference pattern).
 (c) A vertical notch reject filter transfer function.
 (d) Result of filtering.
 (The thin black border in (c) is not part of the data.) (Original image courtesy of Dr. Robert A. West, NASA/JPL.)



a b

FIGURE 4.66

(a) Notch pass filter function used to isolate the vertical axis of the DFT of Fig. 4.65(a).
(b) Spatial pattern obtained by computing the IDFT of (a).

